Paläontol Z (2012) 86:409–439
DOI 10.1007/s12542-012-0129-1

RESEARCH PAPER

# A partial skeleton of *Geotrypus antiquus* (Talpidae, Mammalia) from the Late Oligocene of the Enspel fossillagerstätte in Germany

**Achim H. Schwermann · Thomas Martin**

Received: 22 June 2011 / Accepted: 11 January 2012 / Published online: 10 March 2012


**Abstract** The partial skeleton of a young adult *Geotrypus antiquus* (de Blainville 1840) from the Upper Oligocene (MP 28) found in Enspel comprises the skull with both mandibles, distal ends of both scapulae, left clavicula, humeri, ulnae and radii of both sides, various elements of the hand, some vertebrae, ribs, and the left femur. For the first time, the previously postulated association between dentition and postcranial elements can be confirmed. The skeleton exhibits strong adaptations for a subterranean life, similar to modern fossorial moles. The humerus is wide with a large pectoral process. The wing-like greater and lesser tuberosities, teres tubercle, and distal epicondylus are clearly developed. The metacarpals and phalanges are broad and stout. There are several sesamoid bones in the broad digging hand, including a prepollex (os falciforme). The preserved bones allowed the forelimb of *G. antiquus* to be reconstructed. Previous finds of *G. antiquus* have mainly been from France, with a few specimens from Switzerland and southern Germany. The specimen from Enspel is the northernmost record. A cladistic analysis, based on the matrix of Sánchez-Villagra et al. (Cladistics 22:59–88, 2006), confirms the basal position of *Geotrypus* within the Old World moles (Talpini).

**Keywords** Talpidae · Partial skeleton · *Geotrypus* · Oligocene · Enspel · Germany · Fossorial adaptation · Phylogenetic analysis

**Kurzfassung** Das Teilskelett eines jung-adulten *Geotrypus antiquus* (de Blainville 1840) aus dem Oberoligozän (MP 28) von Enspel umfasst den Schädel mit Unterkiefern, die distalen Enden der Scapulae, die linke Clavicula, sowie die Humeri, Ulnae und Radii beider Seiten, zahlreiche Elemente der Hand, mehrere Wirbel, Rippen und das linke Femur. Da hier erstmalig Gebiss und Humeri eines Individuums assoziiert überliefert sind, kann deren schon früher postulierte Zusammengehörigkeit bestätigt werden. Das Skelett zeigt starke Anpassungen an die subterrane Lebensweise, ähnlich den heutigen fossorialen Maulwürfen. Der Humerus ist breit und hat einen großen Processus pectoralis. Die flügelartigen Tuberositas major und T. minor, Teres major und die distalen Epicondyli sind stark entwickelt. Metacarpalia und Phalangen sind verbreitert und auffallend verkürzt. Die breite Grabhand wird durch zusätzliche Sesamknochen verstärkt, dazu gehört auch ein Präpollex (Os falciforme). Die überlieferten Knochen erlaubten die Rekonstruktion der Vorderextremität von *G. antiquus*. Die bisherigen Funde von *G. antiquus* stammen hauptsächlich aus Frankreich, wenige sind auch aus der Schweiz und aus Süddeutschland bekannt. Der Fund aus Enspel stellt damit den nördlichsten Nachweis dar. Eine kladistische Analyse auf der Basis der Datenmatrix von Sánchez-Villagra et al. (Cladistics 22:59–88, 2006) bestätigt die basale Stellung der Gattung *Geotrypus* innerhalb der Altweltmaulwürfe (Talpini).

**Schlüsselwörter** Talpidae · Teilskelett · *Geotrypus* · Oligozän · Enspel · Deutschland · Grabanpassung · Phylogenetische Analyse

A. H. Schwermann (✉) · T. Martin
Steinmann-Institut für Geologie, Mineralogie und Paläontologie, Nussallee 8, 53115 Bonn, Germany
e-mail: achim.schwermann@uni-bonn.de

## Introduction

Since the early 1990s, the Generaldirektion Kulturelles Erbe Rheinland-Pfalz has conducted excavations in the

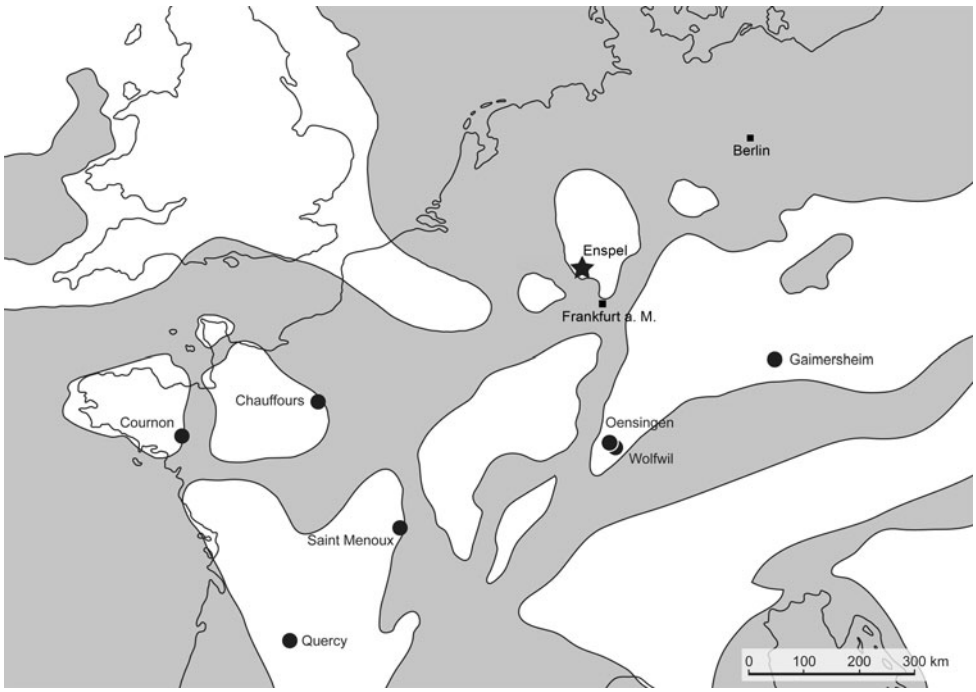


**Fig. 1** Fossil records of *G. antiquus*. Findings that were reported previously are marked with *dots*, and the specimen from Enspel is indicated by an *asterisk* (findings: Crochet 1995; map modified after Ziegler 1990a; Walter 2003)

lake deposits of the Enspel fossillagerstätte (Fig. 1) in the Westerwald, Germany, which date from the Late Oligocene (Wuttke et al. 2010). The lake sediments were deposited in the crater lake of the Stöffel volcano. The volcanic rocks were dated at 24.29 ± 0.05 Ma to 24.56 ± 0.05 Ma (Mertz et al. 2007). The background sedimentation is finely laminated clay interrupted by layers of volcanic ash and siliciclastic sediments, which slipped down from the crater walls (Schindler and Wuttke 2010). A wealth of well-preserved plants and invertebrate fossils has been found since the the excavations were initiated. Among the vertebrate findings, tadpoles of frogs are by far the most abundant, as well as fish (only one species *Palaeorutilus enspelensis* (Böhme 1996)). Other vertebrates such as reptiles, birds, and mammals are rare, and only six mammalian taxa are known from this site (Poschmann et al. 2010). The mole specimen described here has been briefly mentioned previously (Poschmann et al. 2010), but has never been studied in detail before.

Fossils of Paleogene moles mainly consist of isolated teeth, mandibular fragments, or disarticulated bones (e.g., Hugueney 1972; Ziegler 1990b; Crochet 1995), whereas partial skeletons are very rare. The fossil mole from Enspel includes the complete skull with mandibles, the distal ends of the scapulae, the left clavicula, both humeri, both ulnae and radii, various carpals, metacarpals, one os falciforme, a further sesamoid bone, seven vertebrae, three ribs, and the left femur. For the first time, the complete dentition of a Paleogene mole preserved in combination with associated postcranial elements has been found.

The genus *Geotrypus* was described first by Pomel (1848), who also named the species *G. acutidens* and *G. antiquus*. For the latter, he used material first described by de Blainville (1840) as *Talpa antiqua*. The holotype of *G. acutidens* is lost, so *G. antiquus* became the type species of this genus. Since Pomel (1848), several authors have worked with this taxon, describing new species and clarifying the species and genus diagnoses (e.g., Lavocat 1951; Hugueney 1972; Crochet 1995; Ziegler 1990b, and Van den Hoek Ostende 2001). To date, there are eight valid species (Fig. 2) and five unnamed taxa, which are listed in Van den Hoek Ostende (2001). Another unnamed species was described by Ziegler (1985) as "*Talpa*" sp. 1, which was later revised to *Geotrypus* sp. (Ziegler 1994). The known fossil remains of this species-rich genus are from France (Crochet 1974, 1995; Hugueney 1972; Lavocat 1951; Pomel 1848), southern Germany (Tobien 1939; Van den Hoek Ostende 1989, 2001; Ziegler 1985, 1990b, 1994, 1998), Switzerland (Crochet 1995), and Anatolia (Van den Hoek Ostende 2001). The humerus shows the typical broad habitus of a fully fossorial mole, but it is not as wide as in modern true moles (Scalopini and Talpini).

Until now, only a few humeri, fragmentary tooth rows and isolated teeth of *G. antiquus* were known from central and western Europe (Crochet 1995; Lavocat 1951; Pomel 1848) (Fig. 1). Dental and postcranial materials were combined by comparing sizes (Crochet 1995). In general, *G. antiquus* is larger than all other *Geotrypus* species, except for *G. tomerdingensis* Tobien (1939) and *G. kesekoeyensis* Van den Hoek Ostende (2001).

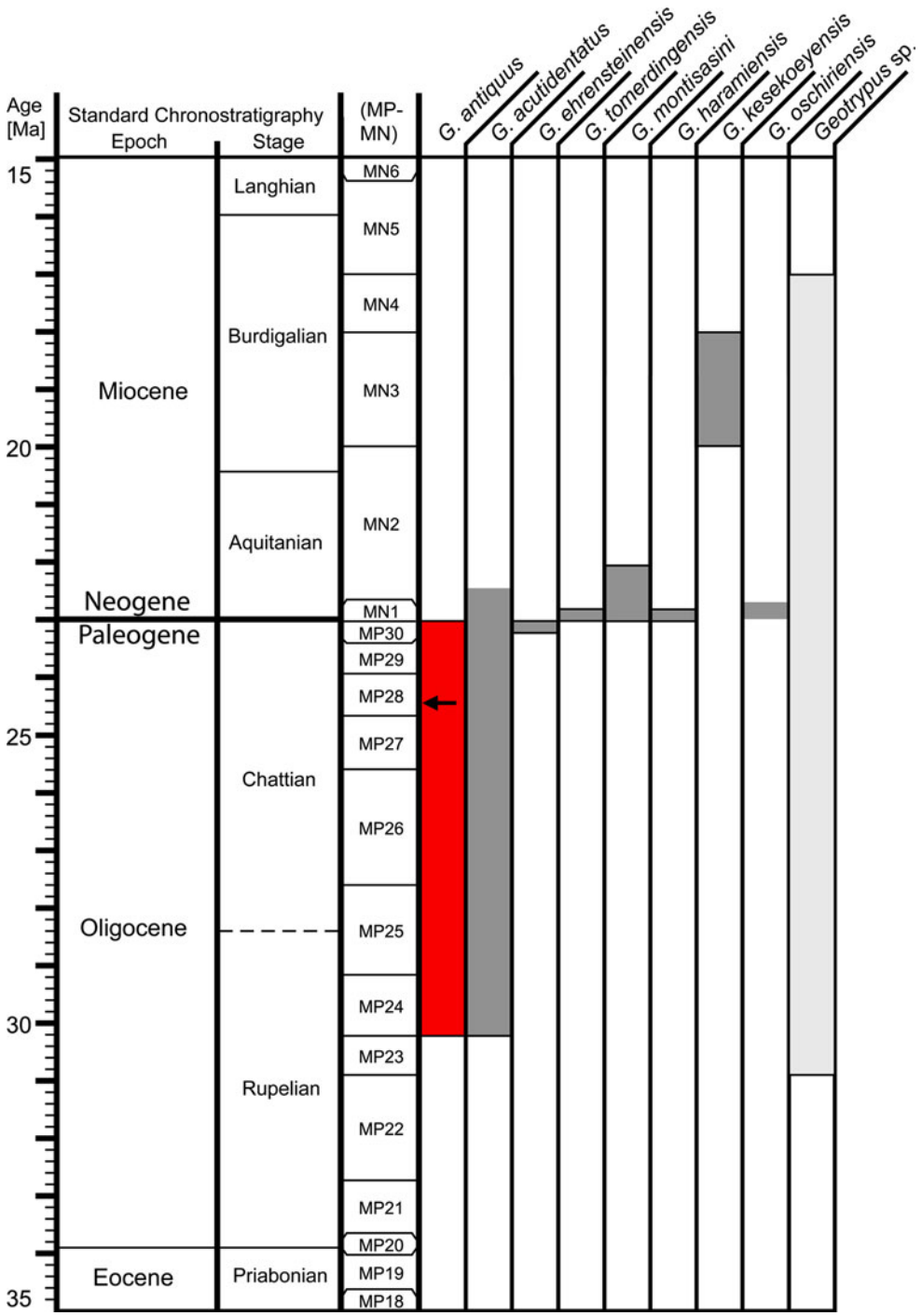


**Fig. 2** Stratigraphic distribution of *Geotrypus* species. The *light gray bar on the right side* marks the extension of the genus, including findings that are only assigned to the genus. The geologically youngest specimen of *G. acutidentatus* was classified by Crochet (1995) to the Aquitanian layer A2 after Aguilar (1982). *G. oschiriensis* from Sardinia is placed in the lowest Miocene, without being classified in a mammal zone. Because of this, these two species are marked with *open bars*. The stratigraphic position of the Enspel specimen is marked by an *arrow*. Created according to data from Crochet (1995), Van den Hoek Ostende (1989, 2001), van den Hoek Ostende and Fejfar (2006), Hugueney (1972), Hutchison (1974), Lavocat (1951), Tobien (1939), Ziegler (1985, 1990b), and Ziegler et al. (2005)

## Materials and methods

The described mole was excavated by the Generaldirektion Kulturelles Erbe Rheinland-Pfalz at the Stöffel basalt quarry near Enspel in 1995. It was found in the excavation debris, but the lithology indicates that it comes from the excavation site G 6, layer S 12. For preparation purposes, the mole was transferred to an artificial epoxy resin matrix and is now exposed from the bottom side. Originally, the animal was lying on the ventral side. The plate has a size of 11.5 × 15.5 cm. The specimen is housed at the Landesmuseum für Naturkunde Rheinland-Pfalz in Mainz (NHMM); its collection number is 1997/PW5145.

In order to perform a complete investigation that included the embedded parts, several $\mu$-CT scans were made with the v|tomel|x s 240 scanner (GE Sensing and

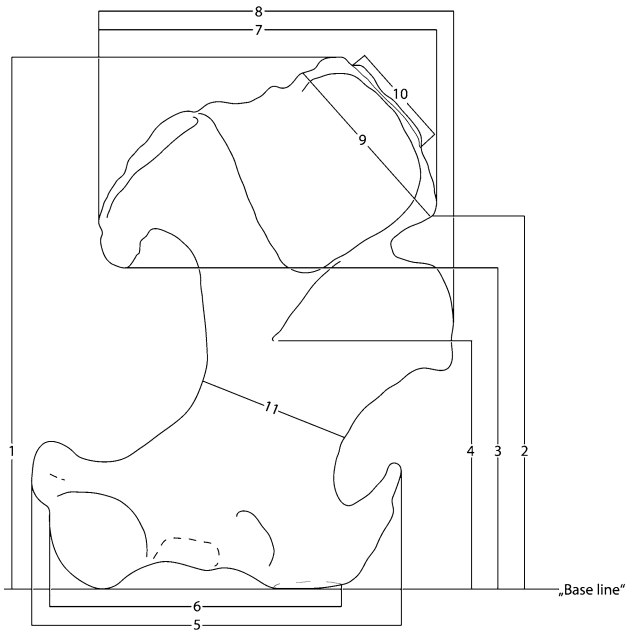


**Fig. 3** Measurements of the humerus (based on Crochet 1995 and Hutchison 1974): *1* 16.4 mm; *2* 12.1 mm; *3* 9.9 mm; *4* 8.5 mm; *5* 11.2 mm; *6* 9.4 mm; *7* 10.1 mm; *8* 11.1 mm; *9* 5.8 mm; *10* 4.4 mm; *11* 4.6 mm; *12* 4.0 mm

Inspection Technologies Phoenix|x-ray) at the Steinmann-Institut. The resolution (isotropic voxel size) was 36–59 µm. The evaluation and digital reconstructions were made with Avizo 6.1. In this way, we performed a complete preparation digitally and nondestructively. Measurements of the humerus (Fig. 3) follow Hutchison (1974, fig. 4) and Crochet (1995, fig. 29). All measurements were obtained with PolyWorks 11 or calipers.

We follow Hutterer (2005) for higher taxonomic classification. Terminology for the dentition, skull, and postcranial skeleton (Figs. 4 and 5) follows Schaller (2007), with additions from Campbell (1939, fig. 15 and 20), and Hutchison (1968, fig. 12 and 14; 1974, fig. 1. and 3). Teeth of the upper jaw are denoted by uppercase letters, and those of the lower jaw by lowercase letters.

Specimens from the Steinmann-Institut Bonn (StIPB M 7003, StIPB M 7089, StIPB M 7090, and StIPB M 7091) and Staatliches Museum für Naturkunde Stuttgart (SMNS 43496, SMNS 44523, and SMNS 43499) were used to compare the mole from Enspel with extant *Talpa europaea* Linnaeus (1758) and fossil *Geotrypus* species.

For the phylogenetic analysis, we used the matrix of Sánchez-Villagra et al. (2006). Their analysis consisted of 157 characters for 17 extant moles and an outgroup of three shrews *Crocidura russula* (Hermann 1780), *Sorex* spp., and *Blarina brevicauda* Say 1823 and the European hedgehog *Erinaceus europaeus* Linnaeus 1758. The mainly dental and osteological characters are divided into 111 binary and 46 multistate traits. Twenty-one of the multistate characters were treated as ordered. Character 70 (height of M1 crown at buccal side/dentary height) could not be coded for *G. antiquus*. For the analysis, a branch-and-bound search was performed using PAUP version 4.0 beta 10 (Swofford 2002). The Bremer support was calculated by heuristic searches of trees of increasing length and a strict consensus for each step.

## Systematic paleontology

Order Soricomorpha Gregory (1910)
Family Talpidae Fischer (1813)
Tribus Talpini Fischer (1813)
Genus *Geotrypus* Pomel (1848)
*Geotrypus antiquus* (de Blainville 1840)

## Osteology

### *Skull and upper dentition*

The ventral side of the elongated skull is visible, whereas the dorsal side is embedded in the resin (Fig. 6). The largest part of the anterior skull is hidden under both dentaries. The maxillary teeth are only partially exposed. The skull is strongly compacted dorsoventrally; the teeth and most of the tooth-bearing parts of the premaxilla and maxilla are the only parts that are not squashed. The occipital condyles at the base of the skull are preserved in their original form. Thin-walled and less massive bone elements are broken but still mark the outline of the skull. The width steadily increases from the anterior to the posterior, similar to the Recent *Talpa europaea*. Jugals and some parts of both squamosals are visible, forming a closed zygomatic arch.

The semicircular canals of the left inner ear lie, in part, under the left squamosum; only small parts of the semicircular canals of the right inner ear are preserved and visible. Other elements of the ear could not be located.

The digital reconstruction of the dorsal skull shows that the individual bone elements are highly intergrown (Fig. 7), similar to the situation in *Talpa europaea*. The nasal opening extends from above the upper canine to just above the incisors, first at an acute angle and then widening at the most anterior edge of the nasal.

The teeth of both maxillaries are preserved, but the molars are partially broken and slightly moved, so it is not possible to reconstruct their roots. The labial side of the left tooth row has been freed from the matrix, but the occlusal surfaces are only partially visible.

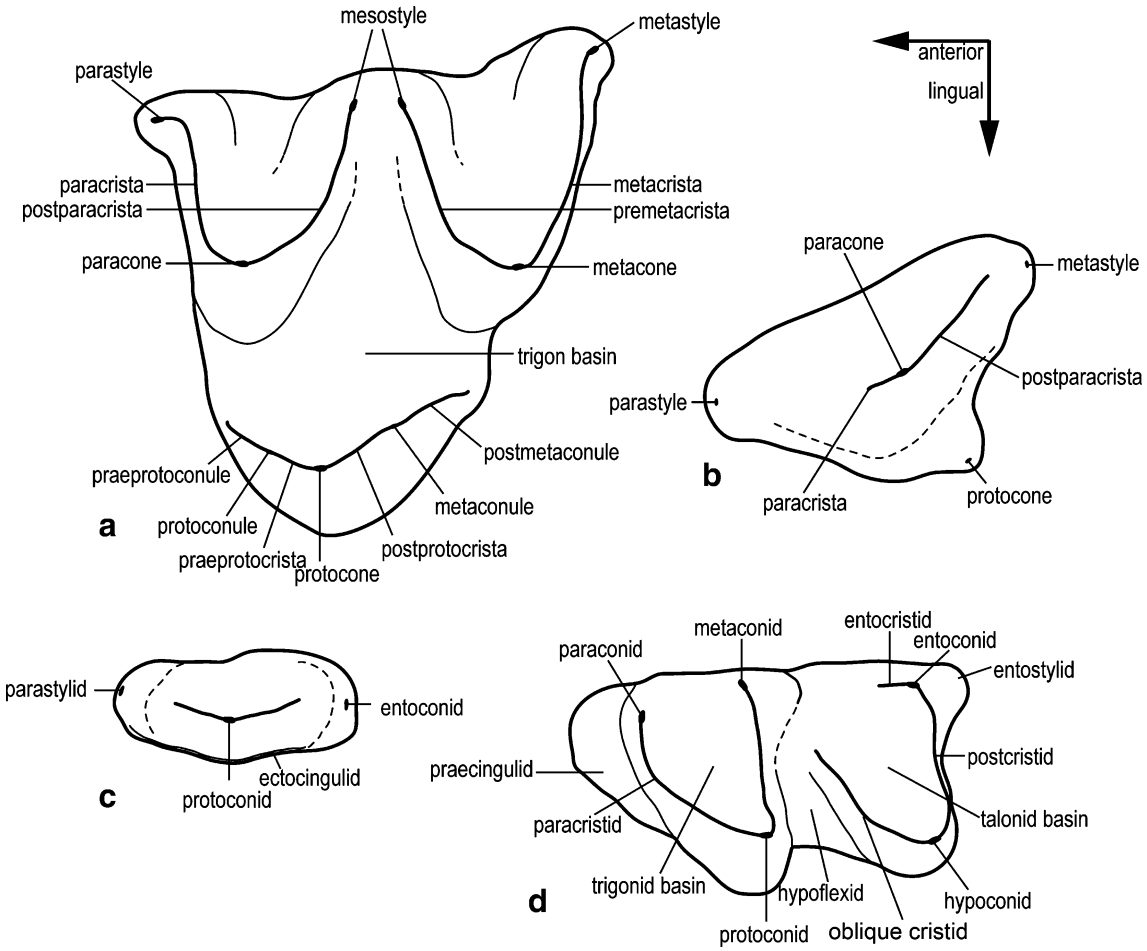


**Fig. 4** Terminology for the dentition (after Hutchison 1974). **a** Upper premolar. **b** Upper molar. **c** Lower premolar. **d** Lower molar

The right maxillary tooth row is only partially visible; the tips of the canine and the ectolophs of M1 and M2 are exposed. All other teeth of the right maxillary are covered by the right dentary. The maxillary tooth formula is 3I C 4P 3 M (Figs. 8 and 9).

The single-rooted incisors are vertically anchored in the premaxilla. Their crowns are long and flat with rounded tips. Furthermore, they are curved slightly to the posterior so that they have a spoon-like shape. Mesially, the two I1 are situated side by side, closely followed distally by I2 and I3. This results in a complete precanine tooth row, with I1 > I2 > I3 (Fig. 8).

The upper canine has two roots of the same size. This tooth is crowding I3 but does not overlap with it. Furthermore, the canine is larger than the incisors and the premolars that follow distally. Due to its size, it assumes the dominant position in the dental sequence of the maxilla. The crown is not wider than the width of the two roots and it has an oval cross-section. Towards the tip, the cross-section becomes smaller and rounder. The tip of the canine slightly curves to the anterior. At the posterior transition from the crown to the root, there is a small, elongated enamel ridge that runs towards the tip of the canine. The canine is followed by a diastema, which is about the length of the canine.

The first three premolars are double-rooted. Unicuspids P1–P3 are relatively simple and morphologically similar. The size of the premolars increases distally: P1 and P2 are approximately equal; P3 is larger than P2, but much smaller than P4 (Fig. 9).

The crown of the first premolar (P1) narrows from the base to the tip of the paracone. The cross-section of the tooth is oval at the crown–root junction to circular at the tip. Posteriorly, there is a weak bulge above the crown base. At this position, metastyli are formed at P3 and P4.

The following P2 is similar in size to P1. P2 also has a metastyle located at the posterior crown base.

Other than in P1 and P2, the posterior section of P3 is slightly concave and develops distally into a sharp edge. The parastyle forms a small bulge mesially. A metastyle is formed in the posterior.

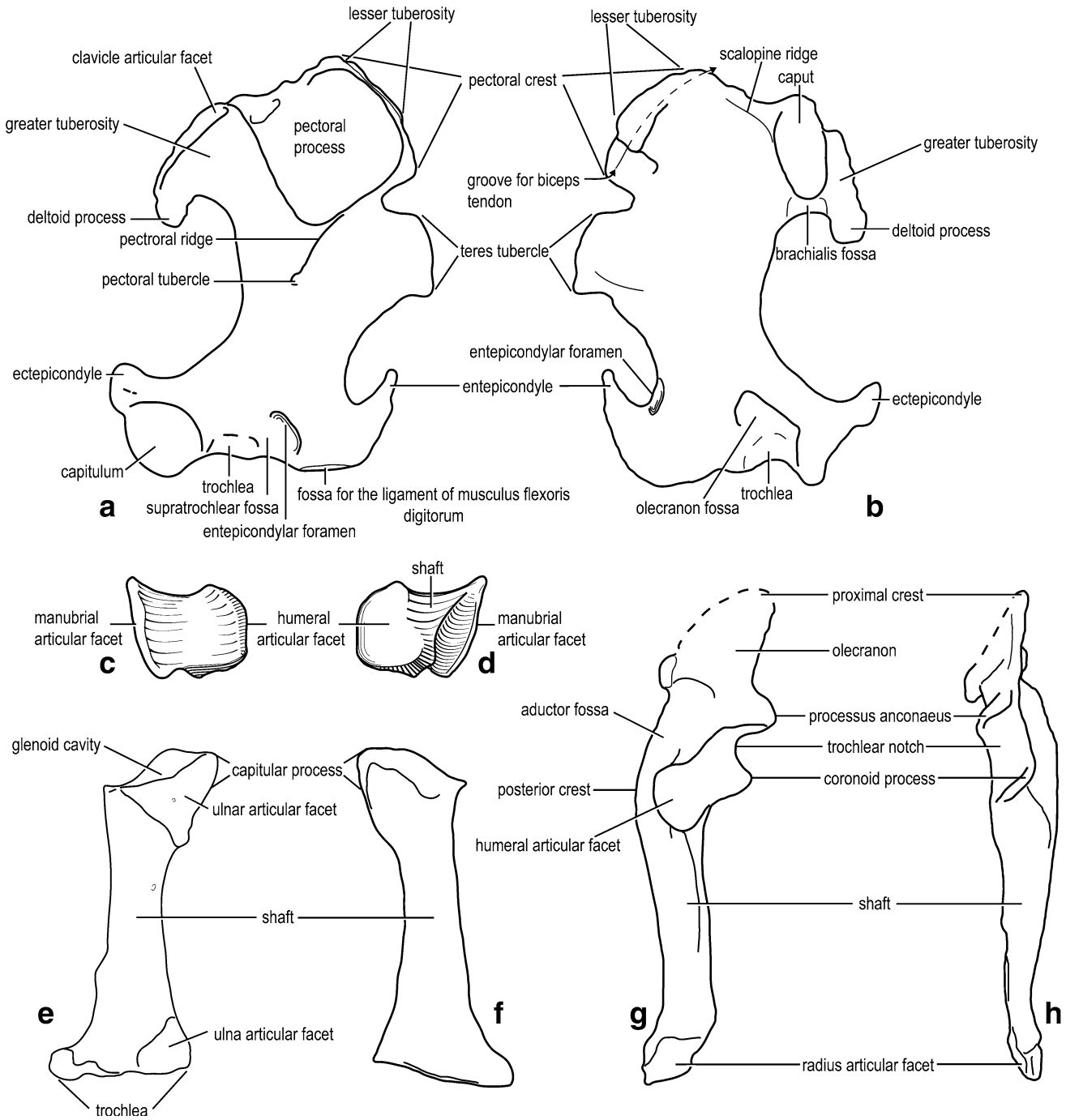


**Fig. 5** Terminology for the humerus, clavicula, radius, and ulna (after Hutchison 1968, 1974). **a** Humerus from anterior. **b** Humerus from posterior. **c** Clavicula from dorsal. **d** Clavicula from ventral. **e** Radius from medial. **f** Radius from lateral. **g** Ulna from lateral. **h** Ulna from anterior

The P4 is the largest premolar. The anterior region has a pronounced parastyle, and there is a well-developed metastyle posteriorly. The labial side of the crown is slightly bent posteriorly, as in P3. The digital reconstruction shows that this tooth has three roots. Two roots are on the labial side, while the third one is positioned lingually. As a result, the base of the tooth is approximately triangular. At the anterior part of the dominant paracone, a postparacrista runs from the tip to the labial root. The small protocone is supported by the lingual root. As in P3, there is a metastyle at the posterior end.

The upper molars show a length ratio of M1 > M2 > M3 (Fig. 9). On the left side, the buccal parts are visible. Because of a rotation due to the compaction of

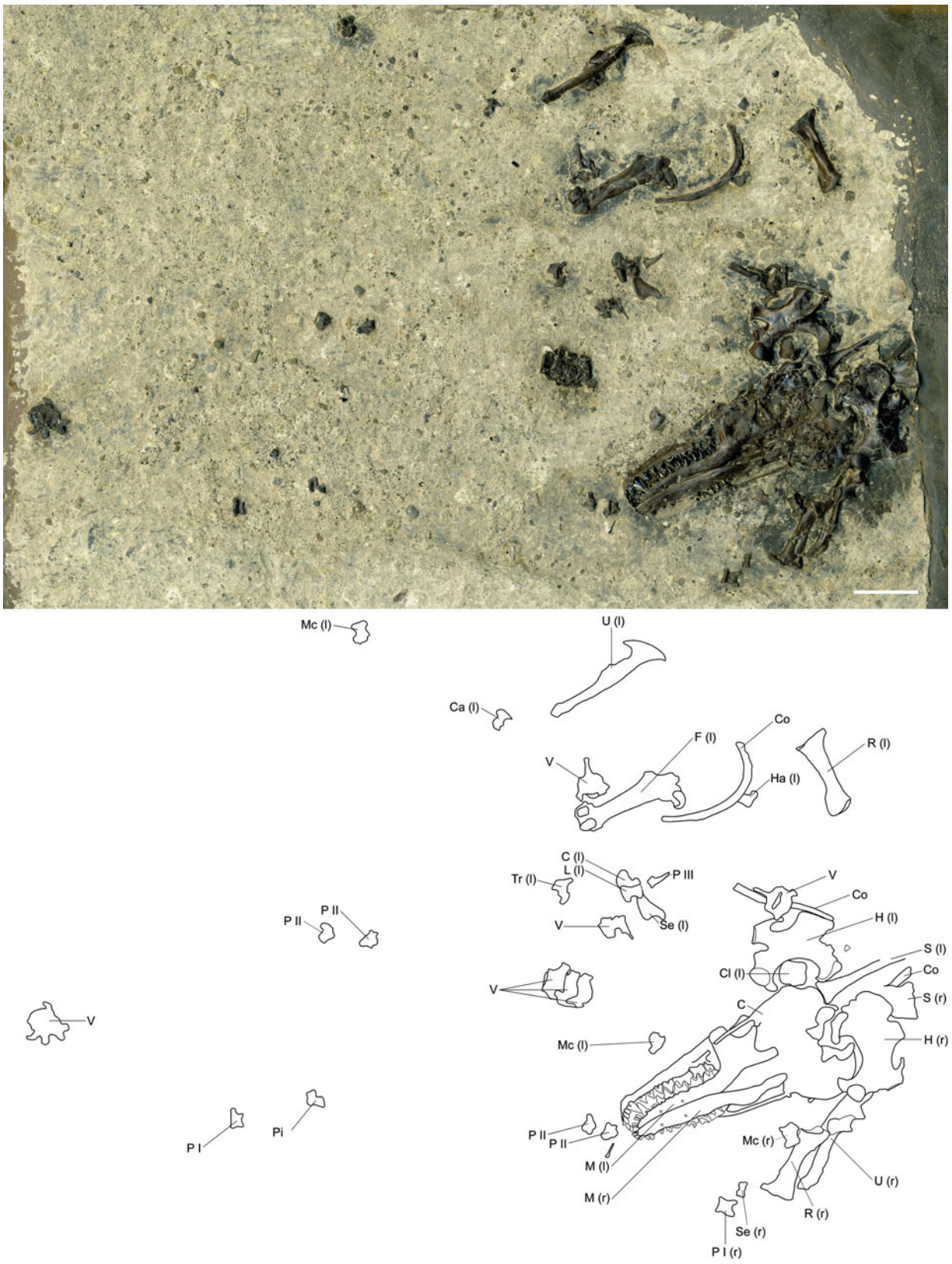


**Fig. 6** The partial skeleton of *G. antiquus* (NHMM 1997/PW5145) from the Upper Oligocene deposits at Enspel. *C* cranium, *Ca* capitatum, *Cl* clavicula, *Co* costa, *F* femur, *H* humerus, *Ha* hamatum, *L* lunatum, *M* mandibula, *Mc* metacarpal, *P* phalanx, *Pi* pisiforme, *R* radius, *S* scapula, *Sc* scaphoideum, *Se* sesamoideum, *Tr* triquetrum, *V* vertebra. *Scale bar* 10 mm

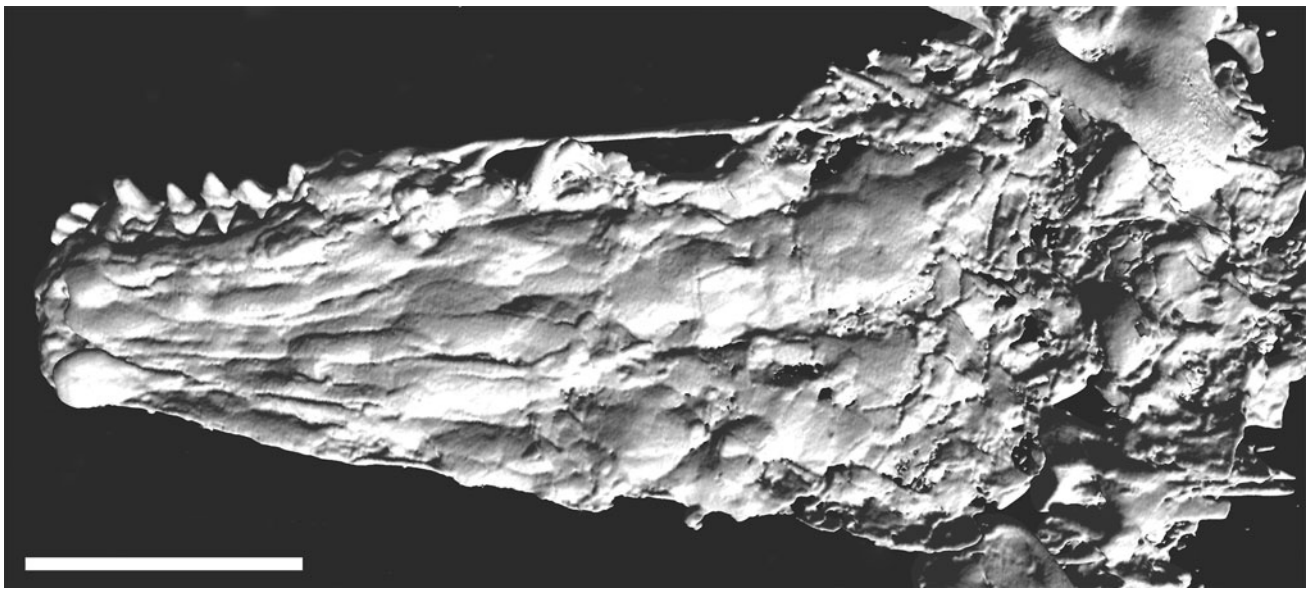

**Fig. 7** Digital reconstruction of the embedded dorsal skull of *G. antiquus* (NHMM 1997/PW5145). *Scale bar* 10 mm

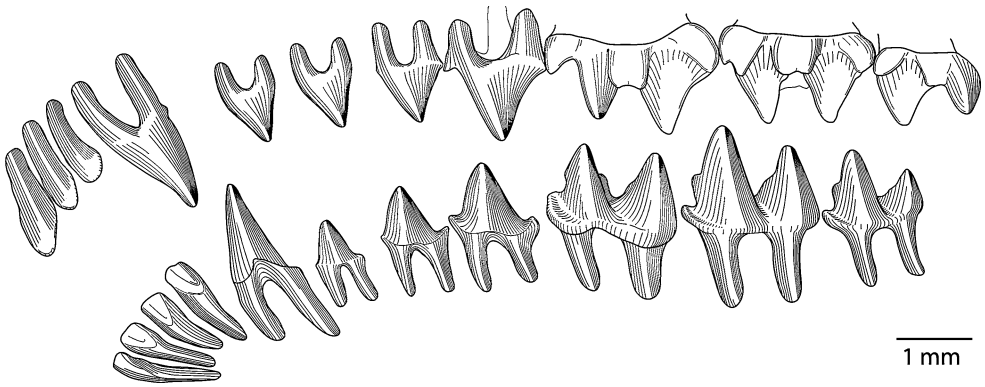


**Fig. 8** Drawing of the reconstructed left dentition of *G. antiquus* (NHMM 1997/PW5145): buccal view

the upper jaw, a partial occlusal view is exposed in M2 and M3. M1 and M2 were slightly deformed by shearing, and the parastyle of M3 is broken off. The lingual sides of the molars are covered by the right lower jaw; only the buccal parts of the three teeth are partially exposed.

The first molar (M1) has a triangular base, with the buccal side being the longest. The posterior outline is pointed, whereas the anterior side is much wider. A buccal ectocingulum is not present. At the anterior end, there is a pronounced parastyle, which is elongated in the mesial direction. The paracone is a solid bump with an approximately circular cross-section. A paracrista is not present, but the postparacrista begins at the bottom of the cusp and leads to the prominent, notched mesostyle. The premetacrista runs horizontally from the mesostyle until the transition point at the metacone. The metacone is the highest structure of the tooth, significantly higher than the paracone, which sits more lingually than the metacone. The metacone cusp is semicircular, with a flattened buccal side. The metastyle is solidly built and extends in the distal direction.

The digital reconstruction of the lingual portion of the protocone, pre-, and postprotocrista shows that the left M1 is badly damaged; the right M1 also has multiple fractures. The substantially raised protocone and the metaconule were fully reconstructed. Since M1 and M2 are very similar in their lingual aspects, we refer to M2 in the description.

The middle molar (M2) is similar in width to M1, but much shorter. It has a triangular shape with a less sharp angle posteriorly than M1. In addition, the paracone and metacone are approximately of equal size. No ectocingulum is present. The parastyle is less pronounced than in M1; the paracrista is separated from the parastyle by only a small notch. The paracrista is well developed, while it is not present in M1. It leads to the paracone, which is similar

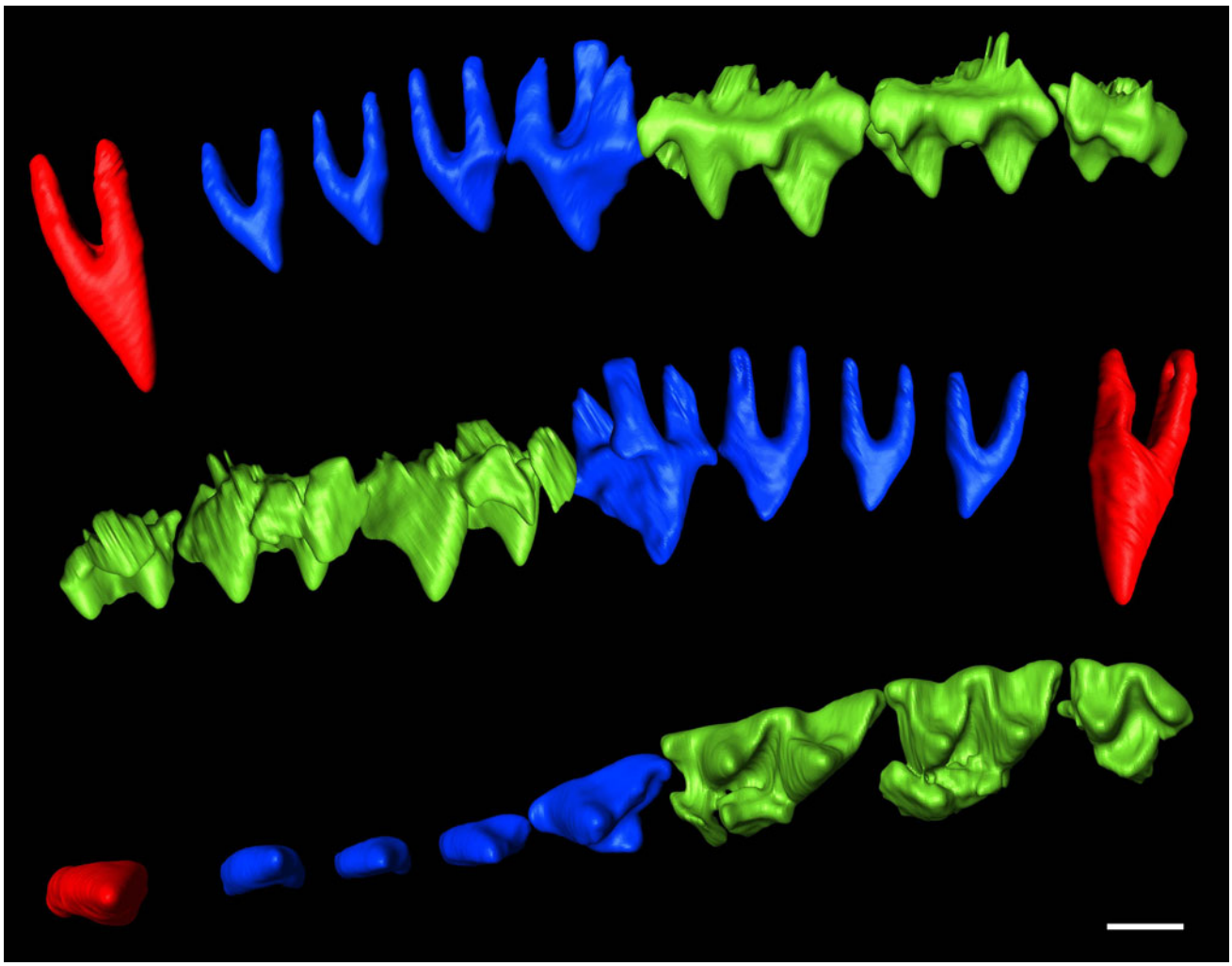

**Fig. 9** Digital reconstruction of the left upper tooth-row without incisors from *G. antiquus* (NHMM 1997/PW5145): buccal (*top*), lingual (*center*), and occlusial (*bottom*) views. Shown are the canine (*red*), premolars (*blue*), and molars (*green*). The lingual parts of M1 and M2 are broken and slightly rotated. *Scale bar* 1 mm

in shape to the metacones of M1 and M2, but more indented lingually. The postparacrista as well as the mesostyle, premetacrista, and metacrista are similar in design to those of M1. The metacone has the same height as the paracone. The posterior metastyle is not as extended as in M1. On the lingual side, a protoconule is slightly developed. It is positioned anterior to the protocone, which is slightly lower than the paracone.

M3 is the smallest of the upper molars. It also has a triangular base that is almost the shape of an isosceles triangle. The tooth shows no cingulum. Anteriorly, there is a small, slightly protruding parastyle; it is separated by a small notch from the paracrista. The arrangement of the paracrista, paracone, and postparacrista is similar to that of M2. The mesostyle is relatively small but also has a shallow notch. The posteriorly following premetacrista is shorter than the anterior cristae and extends to the tip of the small metacone. This is not as high as the paracone and is much narrower. A metastyle does not exist. The lingually situated protocone is large but not as high as the paracone and metacone.

Measurements [mm]: I1–M3 (curved tooth row measured diagonally) = 16.23, P1: L = 0.87, W = 0.54; P2: L = 0.93, W = 0.49; P3: L = 1.20, W = 0.60; P4: L = 2.03, W = 1.27; M1: L = 3.26; M2: L = 2.41, W = 2.67; M3: L = 1.72, W = 1.57.

### *Mandibles*

Both mandibles are completely preserved (Fig. 6). The teeth of the left mandible are in occlusion with the teeth of the left maxilla (Fig. 9). The tooth row of the right mandible is obscured by resin matrix.

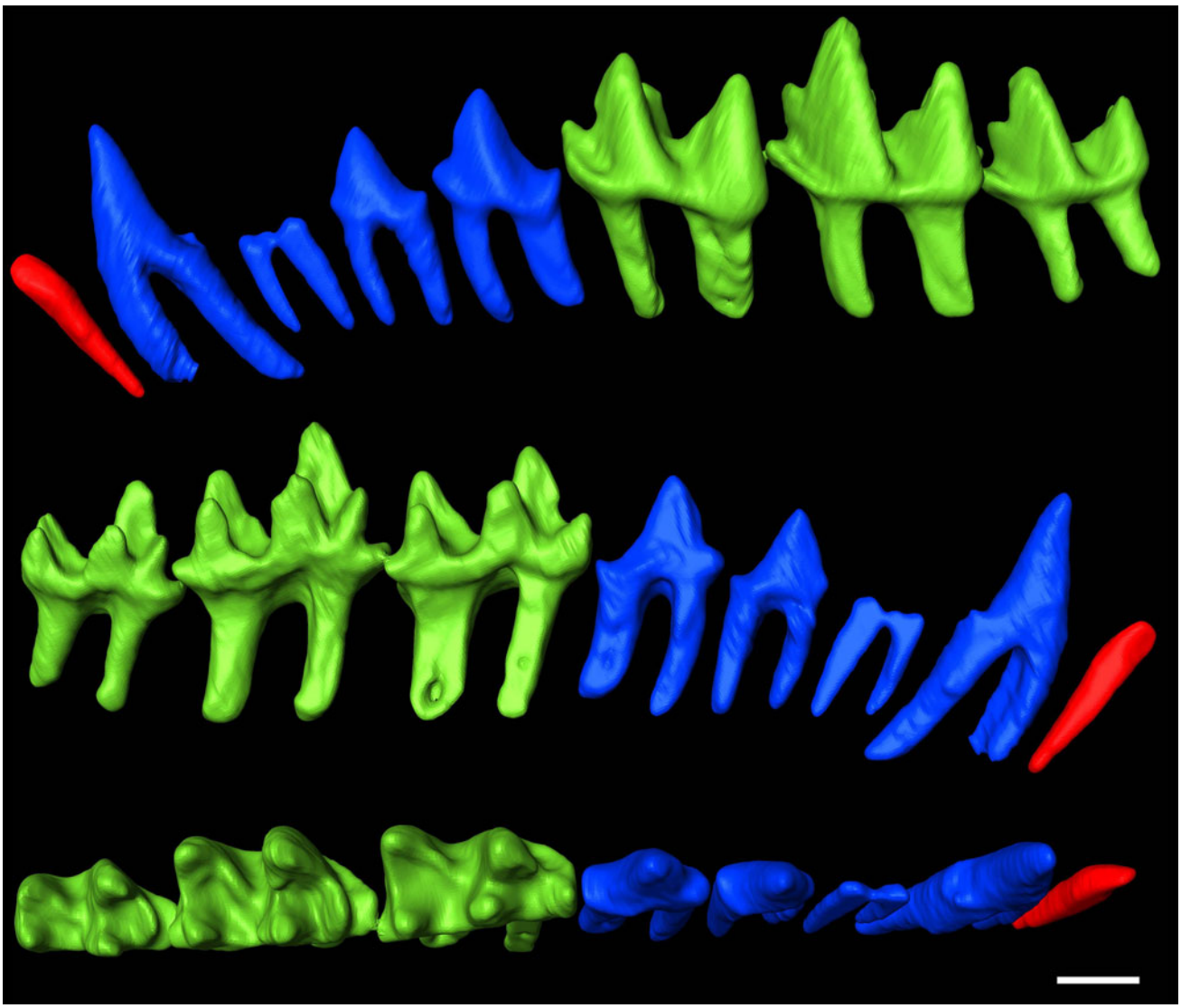

**Fig. 10** Digital reconstruction of the left lower tooth row without incisors from *G. antiquus* (NHMM 1997/PW5145): buccal (*top*), lingual (*center*), and occlusial (*bottom*) views. Shown are the canine (*red*), premolars (*blue*), and molars (*green*). The crown of the left p2 is broken off. *Scale bar* = 1 mm

The corpus mandibulae is slender and elongated with two mental foramina. Their positions are below the interdental area between p2 and p3 and below the anterior root of m1.

The angular process is elongated towards the back; it is in line with the tooth row. The condylar process is positioned above the tooth row and pointed backwards, but it is not as long as the angular process. The articular head of the condylar process is wider than it is long. The coronoid process forms a convex outline, with its highest point being above the middle length of these processes.

The lower incisors are narrow and have a single root (Fig. 8). They are all about the same size, a bit smaller than the antagonists in the premaxilla. Furthermore, they have a spatulate habitus with terminal ends that are not as rounded as in the upper incisors.

The lower canine is small, about the same size as the incisors (Figs. 8 and 10). It is also single-rooted and in line with the incisors.

The caniniform p1 is high and the largest of the premolars (Fig. 10). It is double-rooted, as are all the premolars. A small entoconid is positioned at the base of the crown. The protoconid is high and tapers upwards with a near-circular cross-section at the top. There is a small cingulid at the labial side.

The crown of the left p2 is broken off, but there is a supplement on the right side that could be analyzed by

$\mu$-CT. The smallest premolar has a simple form with an oval cross-section. There is a small entoconid at the posterior base. The protoconid is the dominant cusp; its tip is above the anterior root. A very weak cingulid runs along the labial side.

In comparison to p2, p3 is larger, more differentiated, and complex, a trend that continues in p4. At the front of p3, a parastylid is located at the crown base. The posterior entoconid in p3 is more extended than in p2. The entoconid and parastylid are connected by a narrow, labial cingulum.

The p4 is higher than p3, but not as high as p1. The parastylid and entoconid are clearly developed, and are also connected by an ectocingulid. At the posterior side of the protoconid, a protocrista runs from the tip of the protoconid to the entoconid.

The lower premolars are in line without any imbrications, but with significant interdental spaces (Fig. 10).

The first two lower molars are of a similar size, but m2 is higher than m3. The third molar is not as long nor as high as m1 and m2. The structure of the molars is similar; they all have an elongated base and five cusps.

A precingulum is formed at the anterior end of the teeth, rising toward the lingual side. The protoconid is the highest and most massive cusp. A tall paracristid connects the protoconid and the paraconid. The paraconid is relatively short and wide. It is clearly separated from the metaconid by a notch. The protocrista connects the metaconid with the protoconid. The metaconid and entoconid are separated by a deep incision, which is the deepest point of the lingual occlusion area. A small entostylid is present in m1 and m2, which is relatively high and posterior to the entoconid. In all three molars, the metaconid is higher than the entoconid. The oblique cristid runs from the top of the hypoconid and ends approximately in the center of the tooth. The anterior part of the tooth is separated from the posterior by the hypoflexid.

Measurements [mm]: i1-m3 = 15.09; p1: L = 1.26, W = 0.77; p2: L = 1.04, W = 0.59; p3: L = 1.18, W = 0.64; p4: L = 1.56, W = 0.85; m1: L = 2.46, W = 1.49; m2: L = 2.62, W = 1.51; m3: L = 2.06, W = 1.23; mandible: L = 25.0.

### *Axial skeleton*

All together, seven vertebrae are preserved: three articulated cervical vertebrae, three isolated thoracic vertebrae, and a lumbar vertebra. They are all strongly flattened by compaction.

One complete rib and two rib fragments have undergone heavy compaction. The complete rib is curved at about an angle of 110° and is 22 mm long, similar to the largest ribs in *Talpa europaea*.

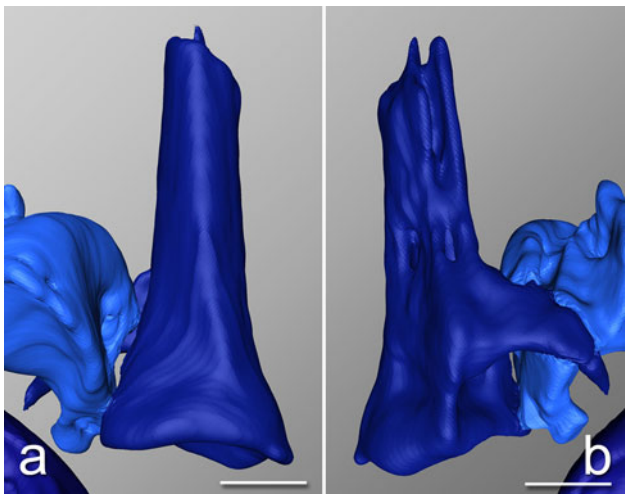


**Fig. 11** Digital reconstruction of the distal left scapula of *G. antiquus* (NHMM 1997/PW5145). The elongated metacromion process is notable. It is shown from ventral (**a**) and dorsal (**b**) views. *Scale bar* 2 mm

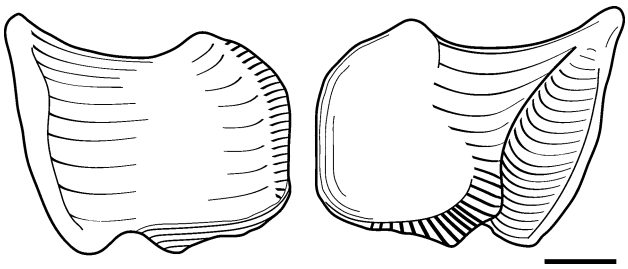

**Fig. 12** Drawing of the left clavicula of *G. antiquus* (NHMM 1997/PW5145) from dorsal (*left*) and ventral (*right*) views. *Scale bar* 1 mm

### *Shoulder girdle*

The distal ends of both scapulae are preserved. The right one lies below the right humerus, so only a small section is visible. The left scapula (Fig. 11) is elongated with a deep, elliptic glenoid cavity at the distal end. The spine runs the entire length of the scapula until its broken proximal end. At the distal end, a small acromion process is present, with a distally broken but still relatively long metacromion process, which tapers towards the distal end.

Only the left clavicula is preserved (Fig. 12) and partially exposed. The digital reconstruction shows a large humeral articulation facet and a similar large manubrial articulation facet, which are connected by the stout shaft. Contrary to modern fossorial moles, this bone is longer than wide in *Geotrypus antiquus*.

Measurements [mm]: glenoid facet: L = 3.4, W = 1.8; clavicula: L = 4.8.

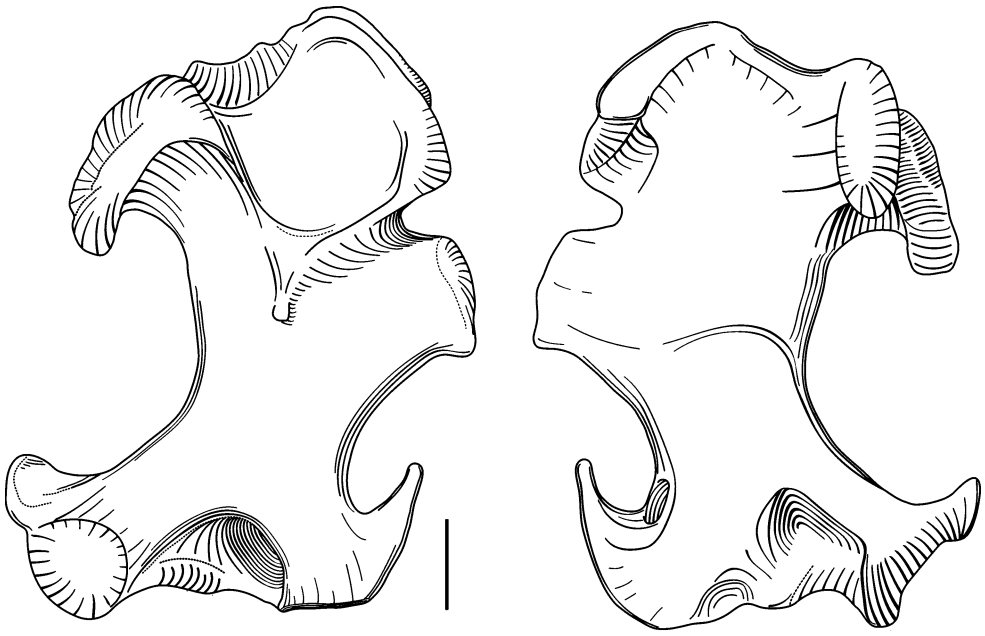

**Fig. 13** Drawing of the right humerus of *G. antiquus* (NHMM 1997/PW5145) from anterior (*left*) and posterior (*right*) views. *Scale bar* 2 mm

*Humeri*

The anterior sides of both humeri are exposed. The right humerus is nearly completely preserved (Figs. 13 and 14), wheres the left one is damaged at the proximal end.

The humerus is very wide compared to the length, which is typical of fossorial moles. Both ends are extremely broad and the connecting shaft is solid and stout. The large pectoral process expands on the anterior side. This depression is limited by the pectoral ridge on the lateral and by the greater tuberosity on the medial side. At the proximal end, the pectoral process has grown together with the lesser tuberosity. Between these runs the groove for the biceps tendon. The lateral outer edge of the lesser tuberosity is about two-thirds the length of the one for the pectoral process. There is a large foramen between the medial pectoral ridge and the greater tuberosity. The greater tuberosity itself is a large process with a terminal clavicula articulation surface. At the distal end of the greater tuberosity, there is a deltoid process directed toward the ectepicondyle. Together, the deltoid process and the ectepicondyle form a large, concave medial outline. The caput has an elliptic outline, as in other fossorial moles. It is the dominant structure at the posterior proximal end of the humerus. Below the caput and the greater tuberosity, there is the deep brachialis fossa.

The cross-section of the shaft midsection is almost circular. Anteriorly, the pectoral tubercle is centered high on the middle shaft. It marks the distal end-point of the pectoral ridge. This ridge runs along the proximal humerus to the distal end of the pectoral ridge. It forms a continuous ridge that separates the shaft from the pectoral process. The teres tubercle is a large extension that branches off the shaft in the medial direction. This results in a notch between the teres tubercle and the pectoral ridge. The teres tubercle is stretched in the longitudinal direction of the humerus, but it is flattened posteriorly, creating a flat semicircular cross-section.

The basin-shaped ectepicondyle is not enlarged; nor does it extend anteriorly. Next to it, the large capitulum forms an ellipse. The anterior part of the trochlea is clearly developed and is very similar to that of *Talpa europaea*. The anterior end of the entepicondylar foramen ends in the deep and wide supratrochlear fossa. The foramen perforates the distal end of the humerus and reappears laterally at the ectepicondyle. The fossa for the ligament of the musculus flexor digitorum at the lateral and distal edge of the humerus is directed distally at a low angle to the long axis of the humerus. It forms an elliptical depression. The ectepicondyle is rod-shaped and proximally elongated.

Measurements [mm]: 1 = 16.4, 2 = 12.1, 3 = 9.9, 4 = 8.5, 5 = 11.2, 6 = 9.4, 7 = 10.1, 8 = 11.1, 9 = 5.8, 10 = 4.4, 11 = 4.6, 12 = 4.0.

*Ulnae*

Left and right ulnae are present (Fig. 6). Because of the elongated olecranon, the ulna is much longer than the radius (Fig. 15). The olecranon is present at the left ulna, but broken at the right one. It widens in the proximo-transverse direction, which results in a very expanded tuber olecrani. The olecranon becomes narrower in the distal direction and runs cranially to the anconeal process. This

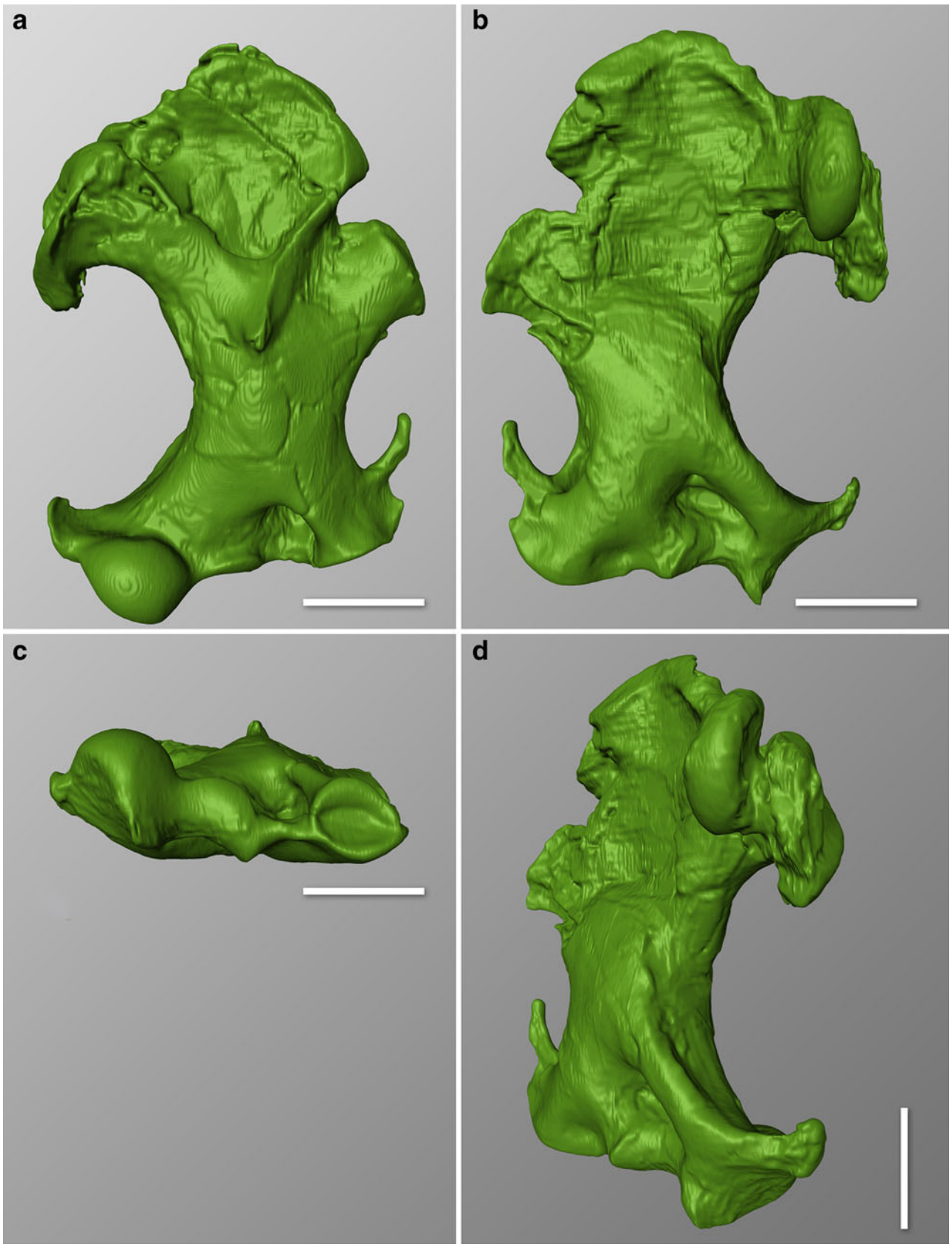


**Fig. 14** Digital reconstruction of the right humerus of *G. antiquus* (NHMM 1997/PW5145): anterior (**a**), posterior (**b**), distal (**c**), and posteriomedial (**d**) views. *Scale bar* 5 mm

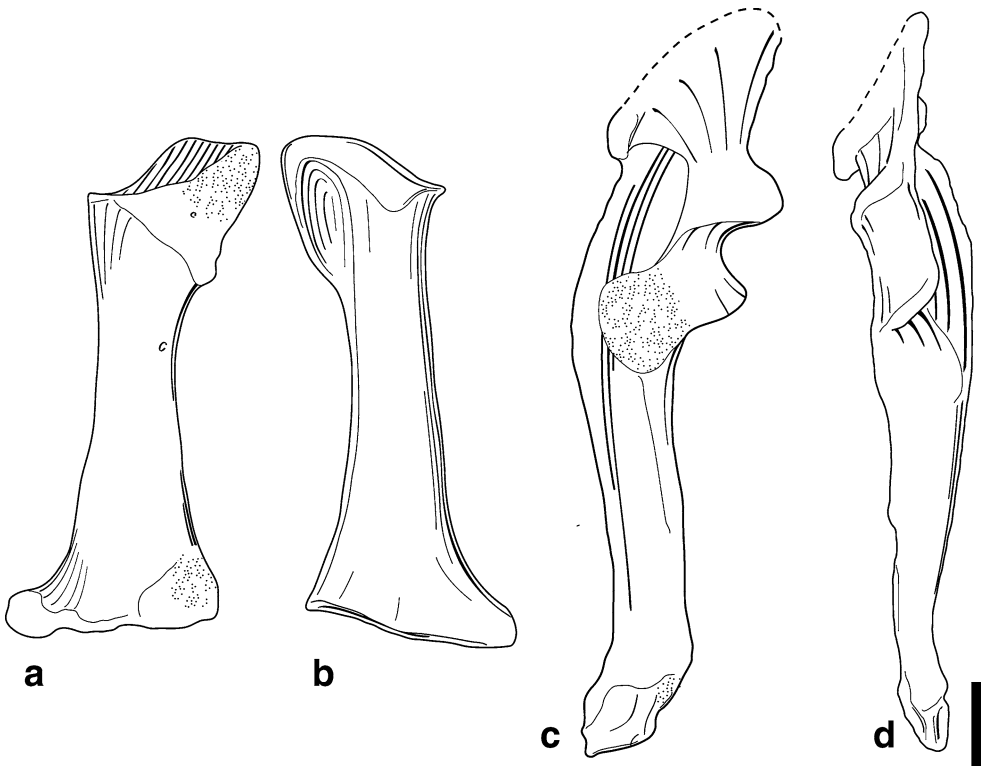


**Fig. 15** Drawings of the radius and ulna of *G. antiquus* (NHMM 1997/PW5145). The radius is shown from medial (**a**) and lateral (**b**) views, and the ulna from lateral (**c**) and anterior (**d**) views. *Scale bar* 2 mm

heavily extended structure is the proximal boundary of the trochlear notch. On the caudal side, the olecranon turns into the adductor fossa, which runs above the shaft for about three-quarters the length of the bone. The coronoid process is the distal boundary of the trochlear notch. The radial articular facet expands towards the laterodistal side, as in *Talpa europaea*. The sinus-like curved shaft tapers towards the distal end. The articular facet of the radius is situated terminally.

Measurements [mm]: L = 20.0; olecranon (from the pivot of the semilunar trochlear notch to the proximal end): L = 7.0.

*Radii*

Both radii are completely preserved (Figs. 6 and 15). The posterior side of the right radius and the anterior side of the left radius are exposed. Proximomedially, a large, triangular articulation facet for the ulna extends proximally above the glenoid cavity, which results in a strong capitular process. The glenoid cavity is deeply concave, allowing it to hold the oval capitulum.

The shaft is not as wide as the caput of the radius. In the lateral view, the ulnar articular facet is supported by a curved bone arch. Together with the shaft, it forms a flat, elongated depression.

The distal trochlea is much wider than the caput. Above the trochlea there is a little articular facet for the distal ulna. The trochlea is elongated medially and laterally, and its articular facets form a channel-like incision.

Measurement [mm]: L = 12.3, proximal W = 4.0, distal W = 5.0.

*Carpals*

Altogether, six different carpalia are preserved (Figs. 6, 16, and 17). By comparing them with the nine carpalia of *Talpa europaea*, they could be identified as the os centrale, os lunatum, os pisiforme, os triquetrum, os capitatum, and os hamatum. The os scaphoideum, os trapezium, and os trapezoideum are not preserved. Apparently, the scaphoideum and lunatum were not fused in *Geotrypus antiquus*, as is the case in extant fossorial moles (Sánchez-Villagra and Menke 2005).

*Metacarpals*

One of the three preserved metacarpals (Figs. 6 and 17) is relatively flat in the dorsoventral direction, with an asymmetric proximal end. It was identified as left Mc V. The second metacarpal is a left Mc IV; it is more stout and not as flat as the first one, and more symmetric at its proximal end. The third metacarpal is very long, with near-rectangular cross-section at its ends. It probably is a right Mc II or Mc III.

Proximally, these bones have a square outline. A short and thickened corpus connects the proximal and the distal ends. The massive, distal joint role is wider than the corpus

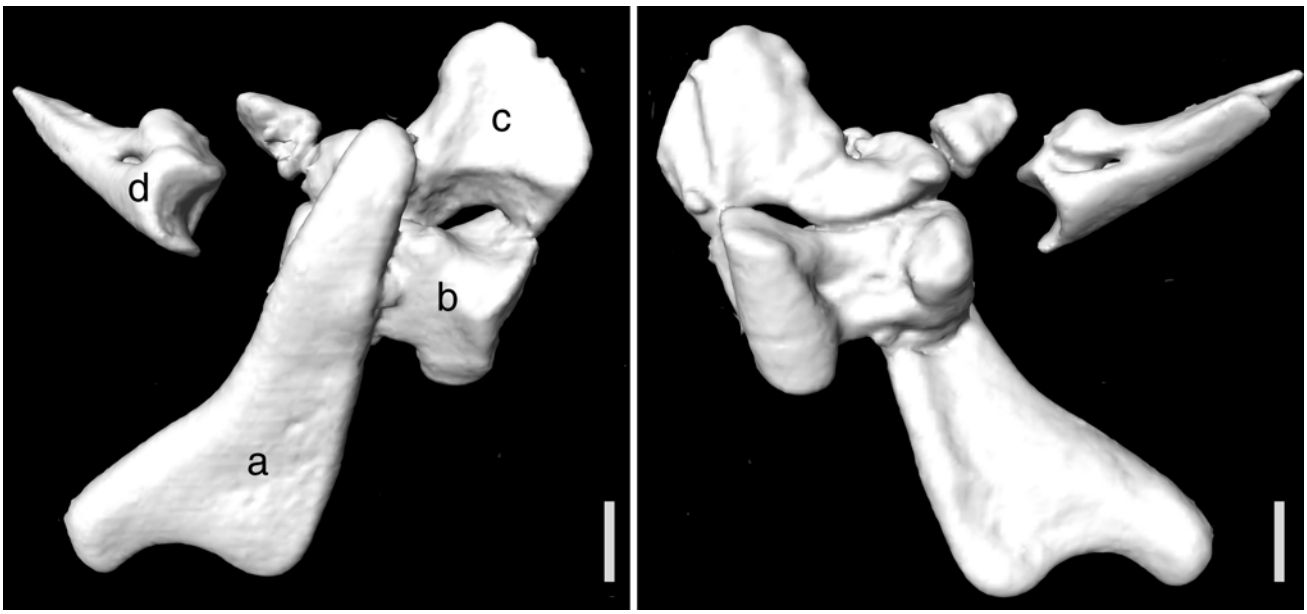


**Fig. 16** Digital reconstruction of the os falciforme (*a*), lunatum (*b*), centrale (*c*), and a terminal phalanx (*d*) of *G. antiquus* (NHMM 1997/PW5145). *Scale bar* 1 mm

and similar to the width of the proximal joint. The lateral metacarpalia are wider than they are thick at the base.

Measurements [mm]: Mc II or III: L = 3.2, proximal W = 2.4, distal W = 2.2; Mc IV: L = 2.6, proximal W = 2.1, distal W = 2.4; Mc V: L = 3.1, proximal W = 2.8, distal W = 2.7.

*Phalanges*

Seven phalanges are preserved on the slab (Fig. 6). Their positions in the fingers—basal, middle, or distal—can easily be determined because of their proportions and symmetries.

The proximal phalanges are shorter than the metacarpalia. They have a wide proximal articular facet, fitting to the round distal joint of the metacarpalia. The corpus is slightly bent toward the palm and leads to the round distal articular facet, which is formed similarly to the metacarpal bones.

The middle phalanges are very short, with a big articular facet at the proximal end and a wide and rounded joint at the distal end. They increase in width from the base to the terminal end.

Lastly, the distal or terminal phalanges are only represented by one specimen (Figs. 6 and 16). Because of its small size, it probably belongs to finger IV or V. Like the other phalanges, it has a wide proximal articular facet. The bone flattens to the broad distal end. There is a still-intact terminal tip on the left side, while the right one is slightly damaged. This suggests that the phalange was terminally split, as in *Talpa europaea*. Two axial foramina are present, one on the lateral and one on the medial side.

Measurements [mm]: P I: L = 1.9, proximal W = 3.0, distal W = 1.8; P I: L = 3.2, proximal W = 3.0, distal W = 2.5; P II: L = 2.7, proximal W = 2.4, distal W = 1.6; P II: L = 2.7, proximal W = 2.5, distal W = 1.3; P II: L = 2.3, proximal W = 2.8; distal W = 1.7; P II: L = 2.8, proximal W = 2.5, distal W = 1.4; P III: L = 3.8, W = 1.3, H = 1.5

*Sesamoid bones*

Two sesamoid bones are preserved (Fig. 6). In extant *T. europaea*, there are a number of sesamoid bones on the volar side of the hand skeleton between the metacarpalia and the first phalanges of each finger. Some of them are flat and have a rectangular shape, like one of the bones in the Enspel skeleton.

The second sesamoid bone of the Enspel specimen was identified as an os falciforme (Fig. 16). It is large, similar to that of *T. europaea*, but not as strongly curved.

Measurements [mm]: sesamoid bone: W = 4.8, H = 2.5; os falciforme: L = 8.0. The preserved bones of this specimen allowed the forelimb of *G. antiquus* to be reconstructed in a digital way (Fig. 17).

*Femur*

The left femur (Fig. 18) is the only preserved element of the hind leg. It is heavily compacted and only

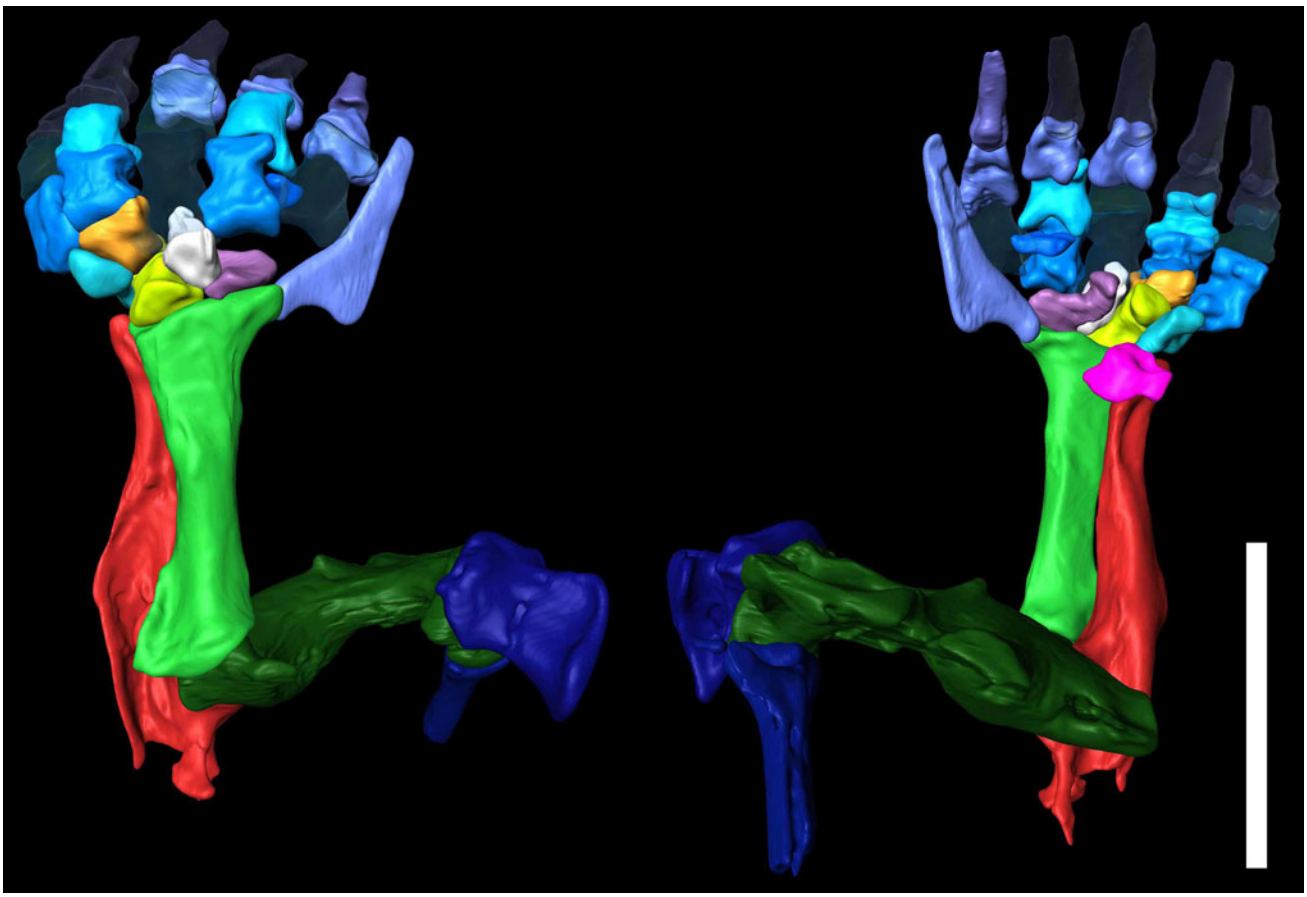

**Fig. 17** Digital reconstruction of the left forelimb skeleton of *G. antiquus* (NHMM 1997/PW5145) from dorsal (*left*) and volar (*right*) views. Preserved bones are shown *opaque*, additions are *transparent*. Humerus, radius, ulna, os pisiforme, metacarpal of the second finger, and the sesamoid bone between the metacarpal and the basal phalanx in the second finger are from the right arm; they were mirrored for this reconstruction. *Scale bar* 10 mm

visible from the plantar side. The caput is oriented in the lateral direction. The plantar side of the greater trochanter is divided into a cranial part and a caudal part, which is positioned laterally. There is a convex notch between them. The slender shaft is elongated and shows no further differentiation. Distally, it widens to the lateral and medial epicondyles, which are divided by the intercondylar fossa. The anterior aspect shows a generalized femur, similar to *Talpa europaea*.

Measurements [mm]: L = 17.0, proximal W = 5.4, distal W = 4.2.

### Phylogenetic analysis

Phylogenetic analyses of extant moles were performed by Whidden (2000) using myological features, and by Motokawa (2004) using craniodental features. Shinohara et al. (2003, 2004) based their analyses on mitochondrial DNA cytochrome b, and Sánchez-Villagra et al. (2004, 2006) and Sánchez-Villagra and Menke (2005) used dental and osteological characters.

We used the matrix of Sánchez-Villagra et al. (2006), which is based on dental and osteological characters, and added the character codings of *Geotrypus antiquus* (see Appendices 1 and 2). The result was one most parsimonious tree (TL = 482, CI = 0.45, RI = 0.66; RC = 0.30) with a similar topology to the only extant mole tree of Sánchez-Villagra et al. (2006) (Fig. 19). The monophyly of Talpini was confirmed by our analysis, and the assignment of *Geotrypus* to this taxon was supported. *Geotrypus* fits at the base of this Eurasian clade of highly fossorial moles.

## Discussion

### Taphonomic aspects

A typical carcass takes a relaxed posture in the water (Weigelt 1927), which was observed in other vertebrate

**Fig. 18** Strongly compacted left femur of *G. antiquus* (NHMM 1997/PW5145) from the posterior view. *Scale bar* = 1 mm

fossils from Enspel (e.g., *Palaeortyx* cf. *gallica*, Mayr et al. 2006; *Eomys quercyi*, Storch et al. 1996; *Amphilagus wuttkei*, Mörs and Kalthoff 2010). This type of preservation is usually connected with a complete skeleton. Mörs and Koenigswald (2000) described a different case of preservation for the partial skeleton of *Potamotherium valletoni* from Enspel. This skeleton had decomposed before its final deposition at the bottom of the lake.

The mole was lying on its ventral side, which is an unusual posture for a carcass in water. Koenigswald and Wuttke (1987) mentioned this for some mammals from Messel, such as pangolins, which have anatomical specializations that influence their center of gravity. Usually mammalian carcasses are embedded in the lateral position. The position of the mole, lying on its ventral site, is ascribable to its very specialized shoulder girdle and forelimb.

The partial skeleton of the mole includes mainly anterior elements. The skull and mandibles are largely in original articulation. The right arm, with the humerus, radius, and ulna, is preserved in anatomical order but the bones are slightly displaced in their direction to the body axis. The left arm is more disarticulated and the bones were moved away from the body in the lateral direction. The smaller and lighter carpalia, metacarpalia, and phalanges are scattered over a longer distance, mainly in the anterior and sinistral directions. Similarly, the vertebrae, ribs, and femur are moved in the anterior and sinistral directions. Perhaps these disarticulations were caused by a water flow event that mixed up the bones.

The completeness of the skeleton, with the skull and mandibles, mostly complete forelimbs and some parts of the posterior skeleton, indicate that the body was deposited complete or nearly complete. Probably more bones were preserved originally but were lost due to the breakage of the slab.

In contrast to other mammals from Enspel, such as *Amphilagus wuttkei* and *Eomys quercyi* (Mörs and Kalthoff 2010; Storch et al. 1996), no soft tissue is preserved in the mole specimen.

## Ontogenetic stage

There were no previous studies on the ontogenetic development of the genus *Geotrypus*. This is mainly due to the limited fossil record. The individual age of the specimen of Enspel was estimated by comparing it with the extant *Talpa europaea*. Kindahl (1957) observed that the deciduous teeth of *T. europaea* are replaced very early. The milk teeth do not break through the gums and are replaced after the first days of life by the permanent teeth. The Enspel mole has no milk teeth, and it has no open epiphyseal sutures. These are characters of an adult animal. Another indicator of age is the amount of wear on the dentition. Skoczén (1966) investigated the gradual wear stages of *T. europaea* and demonstrated that there is a gradual increase in the number and surface area of wear facets. The first wear facets appear at an age of about three months. There are no visible facets on the teeth of the specimen from Enspel, so it was assigned to a group called the ''young-of-the-year'' (defined by Skoczén 1966)—a young adult animal a few months of age.

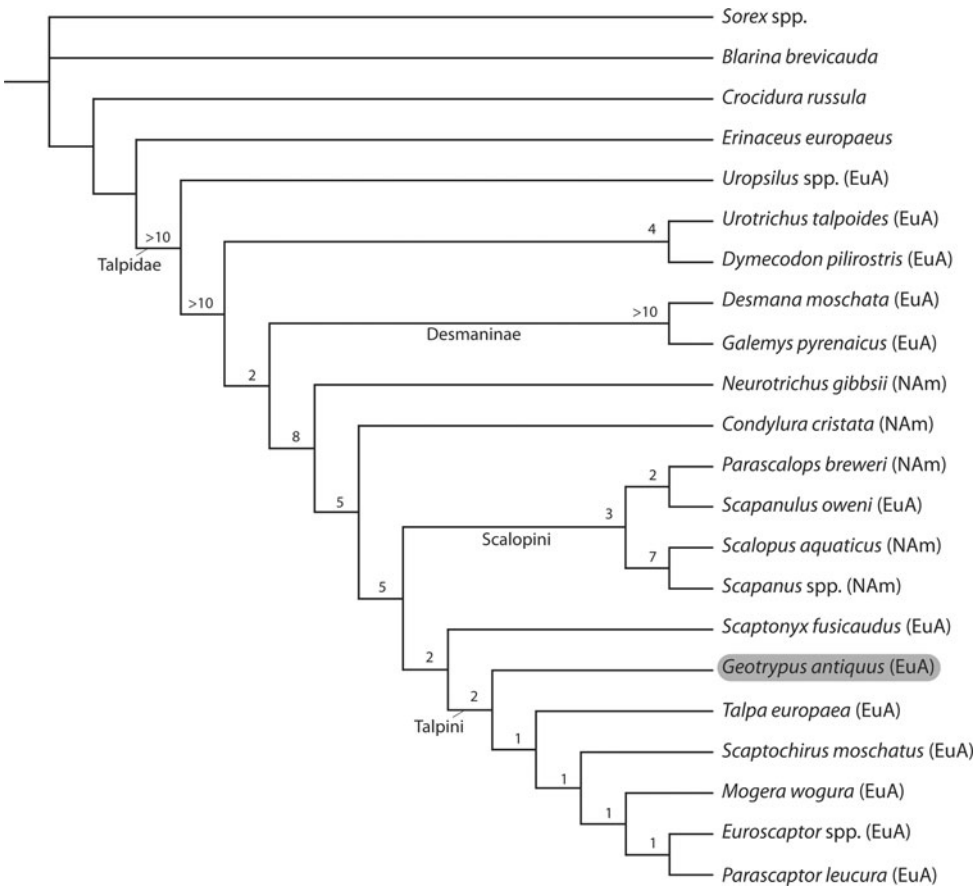


**Fig. 19** Most parsimonious tree (157 characters; TL = 482; CI = 0,45; HI = 0,55; RI = 0,66; RC = 0,30) resulting from a PAUP branch-and-bound-analysis, based on the matrix of Sánchez-Villagra et al. (2006). *Numbers above the nodes* indicate the Bremer support. (*EuA* Eurasia, *NAm* North America)

## Taxonomy and phylogenetic analysis

Many skeletal features including the habitus of the humerus support the hypothesis that *Geotrpus antiquus* belongs to the highly fossorial moles, which are characterized by wide and compact humeri. *Geotrypus* has a wide humerus, not as wide as in modern Talpini and Scalopini, but much wider than in basal talpids, such as Condylurini, Desmanini, Neurotrichini, or Uropsilinae (Campbell 1939).

Besides the *Geotrypus* specimen described here, *G. montisasini* Ziegler (1990b) from Ulm-Westtangente (SMNS 44523) is the only other partial *Geotrypus* skeleton; that partial skeleton comprises most of the upper and lower teeth, parts of the skull with the mandibles, and elements of the forelimbs. Another *G. montisasini* specimen, from Haslach (SMNS 43499), comprises the scapula, humerus, radius, and clavicula, all very likely from one individual.

All valid species of *Geotrypus* were compared to the Enspel mole, three of which are known from the Oligocene.

The Oligocene taxa are *Geotrypus antiquus* (de Blainville 1840), *G. acutidentatus* (de Blainville 1840), and *G. ehrensteinensis* Ziegler (1990b). Only *G. antiquus* and *G. acutidentatus* are expected for MP 28, as *G. ehrensteinensis* is only known from MP 30.

The Miocene species can also be excluded by morphological characters. Four species differ in the dental formula. One or more tooth positions are reduced in *G. acutidentatus*, *G. ehrensteinensis*, *G. montisasini*, and in *G. haramiensis* Van den Hoek Ostende (2001). *Geotrypus tomerdingensis* (Tobien 1939) from the basal Miocene has a very large humerus, 12–48% larger than that of *G. antiquus* and those of the Enspel mole. Another large species is *G. kesekoyensis* Van den Hoek Ostende (2001) from Anatolia. It is only known by its teeth, which are larger than those of the other described species. Finally, *G. oschiriensis* de Bruijn and Rümke (1974) from Sardinia is a rarely documented species with a very short and wide M2. Its assignment to *Geotrypus* is questionable (Crochet 1995; Van den Hoek Ostende 2001).

Both the size of the humerus and the dental formula are crucial to the assignment of the specimen to *G. antiquus*. This is the only known *Geotrypus* species with complete eutherian dentition. Furthermore, its stratigraphic position fits the known record of this species.

Some features differentiate *Geotrypus* from other true moles. The greater tuberosity ends terminally and not, as in Talpini or Scalopini, in an enlarged facies articularis, which merges anteriorly with the humeral shaft. It looks

more like the greater tuberosity in *Neurotrichus* or *Condylura* (Campbell 1939). Furthermore, a foramen on the anterior side is situated between the greater tuberosity and pectoral ridge. This is also observed in other *Geotrypus* species (e.g., *G. tomerdingensis*, SMNS 43496; *G.* aff. *montisasini*, SMNS 45103, 44485; *G. montisasini*, SMNS 43499), but is not documented for extant true moles.

In comparison to the shoulder girdle of extant moles, described by Campbell (1939), the clavicula of *G. antiquus* from Enspel seems to be very long for a fossorial mole. A metacromion, which is present in *G. antiquus*, is not documented for extant, highly fossorial moles. It only appears in basal forms like *Galemys*, *Condylura*, or *Neurotrichus* (Campbell 1939; Reed 1951).

The specimen from Enspel is the first fossil mole with a documented os falciforme. This bone was previously only found in extant taxa (Sánchez-Villagra et al. 2006; Mitgutsch et al. 2011).

More than half of the characters used by Sánchez-Villagra et al. (2006) were coded for *G. antiquus*. There are no changes in the topology of the tree after adding this fossil taxon. Therefore, the previously discussed assignment of *Geotrypus* to the Talpini (Ziegler 1990b; Van den Hoek Ostende 2001) is supported. Furthermore, the position of *Geotrypus* at the base of this Eurasian taxon corresponds to its evolutionary and stratigraphic position.

A phylogenetic analysis of other fossil moles is desirable but remains difficult due to the fragmented documentation of the extinct taxa.

## Conclusion

Because of its stratigraphic position and diagnostic features of the dentition and humeri, the partial skeleton of the mole from Enspel was identified as *G. antiquus*. The fossil record of this species was limited to France, Switzerland, and southern Germany, but has now been supplemented by this northernmost specimen.

A phylogenetic analysis of extant moles and *G. antiquus* results in one most-parsimonious tree with *Geotrypus* as a basal representative of Talpini. This position of *G. antiquus* was postulated earlier (e.g., Ziegler 1990b; Van den Hoek Ostende 2001), and has now been confirmed by cladistic analysis.

Preservation of the skeleton indicates that the mole was deposited complete and was partially disarticulated later.

The specimen represents the most complete skeleton of a Paleogene mole. *Geotrypus antiquus* was a fully fossorial mole with a highly evolved forelimb skeleton. Special adaptations of the hand for digging include stout metacarpals, carpals, and phalanges, and additional sesamoid bones.

Further research should concentrate on the evolution of the shoulder girdles and forelimbs of extant and fossil moles. A comparison of fossil Talpini and Scalopini would be very useful for detecting possible convergent developments in the adaptation to a fossorial lifestyle.

**Acknowledgments** We thank Dr. Michael Wuttke at the Generaldirektion Kulturelles Erbe Rheinland-Pfalz in Mainz for providing the fossil specimen and for information on the excavation and locality. Dr. Irina Ruf, Dr. Julia Schultz, and Peter Göddertz helped with the micro-CT analysis. We thank Georg Oleschinski for the photos of the specimen. Furthermore, for their discussions and helpful suggestions, we thank Dr. Lars van den Hoek Ostende (National Museum of Natural History Naturalis, Leiden) and Dr. Reinhard Ziegler (Staatliches Museum für Naturkunde Stuttgart). We also express special thanks to Jessica Mitchell for her linguistic corrections of the manuscript.

## Appendix 1

Data matrix of the phylogenetic analysis, based on Sánchez-Villagra et al. 2006, including *Geotrypus antiquus*.

Poymorphic entries: a = (01), b = (02), c = (12), d = (23).

"?" = missing data.

| | |
|---|---|
| *Uropsilus* spp. | 00011110?0 2100001111 000111000a 020011a1a1 001c1000a2 010000a100 0101102000 0000010010 1110001201 1000100?00 0010001??0 2000100000 1001??1000 0001000001 1201001110 0?00?10 |
| *Desmana moschata* | 1111111100 2110001133 0010110000 0200000111 1011100001 0101010012 0110212000 1010020111 201?011201 1101101010 0111101100 0010100101 1102?11012 0201101211 1300?????? ?1??100 |
| *Galemys pyrenaicus* | 1111111110 2111001133 1100110001 0100000101 0011100001 0101010011 0111212100 0?10a20a11 2010001201 1101101010 0111101?12 0000100101 1102311012 0211101211 130071??1? ????120 |
| *Scaptonyx fusicaudus* | 1101111111 0111001121 0100010112 1000000110 0112200011 1101122102 0101011111 ??01020011 00?1????12 0?011???d1 ??1110???? ?????????? ?????????? ?????????? ?????????? ??????1 |
| *Talpa europaea* | 1111111111 2110101112 0100110012 100000011000 12100121 1101122102 0201111111 0012020001 0022010012 0201111031 0011112113 1101111010 0002311010 0011000101 0200112011 0110a01 |
| *Scaptochirus moschatus* | 1111100111 2110100122 0100110112 1011000110 0011100121 0101010110 0a01110001 001??2???? ?????????? ?????????? ?????????? ?????????? ?????????? ?????????? ?????????? ??????1 |
| *Euroscaptor* spp. | 1111111111 2111101122 0100110012 100000011a 001110aa21 11011cc111 0200111111 ?1?2120001 0022010012 0201111031 0011112113 010111???? 00?2310110 0011101201 1200111011 0111?01 |
| *Mogera wogum* | 1101111111 2110101122 0100110012 1000000111 0011100021 1111110111 0201111101 0112120001 0022110012 0201111031 0011112113 1101111210 0002311012 0011001101 1201121011 0111101 |
| *Parascaptar leucura* | 1111101111 2111101122 0100110112 1000000111 0011101021 1101121111 110101bc11 ?????20??? ??2???????? ?????????? ?????????3 ?????0???? ?????????? ?????????? ?????????? ??????1 |
| *Urotrichus talpoides* | 0001000110 210000111c 1101010000 0200000101 0011100001 0111112102 0100111100 1000a20011 002001a001 1101111021 0111101312 011010???? ??01111010 1001001200 12?0111010 0011011 |
| *Dymecodon pilirostris* | 0001100110 2100001111 1001010000 0200000101 0012100001 1111122102 0100c12110 0000020011 002010a101 1101101??1 0111?0131? 11?0100110 ?00???1010 0201000210 1201121110 0?01011 |
| *Neurotrichus gibbsii* | 1110000110 1110100112 0010110110 1200001111 0001100011 1101122102 0201111110 1001020011 10211?1?11 1201101021 1111001112 0110100000 1101211112 0a010012a1 1201111011 0111111 |
| *Scapanulus oweni* | ?????11110 2110000133 0101100100 0201000111 0012110001 1101111112 020?012111 ??02021111 002?????12 0?01111?d1 0?11112?1? ?????????? ?????????? ?????????? ?????????? ??????? |

| | |
|---|---|
| *Parascalops breweri* | 1111111100 2101001133 0101100100 0200000011 0021110011 1101112112 0201011111 0?02021111 0022010012 0301111031 0011112213 0100110110 1102311112 0001101111 1200111011 0120111 |
| *Scalopus aquaticus* | 1110011100 0100010033 0001110100 0201000111 0121100001 1111022102 0200212111 1012120111 0023010012 0301111131 0011112213 1100101210 0002311111 0101101010 1200111011 0021021 |
| *Scapanus* spp. | 1111111100 0101010133 0101110101 0200000111 0021100011 1111012102 0200112111 1012020111 002301?011 0301111131 0011112213 0100101210 0002311110 0101000201 0201111011 0121121 |
| *Condylura cristata* | 1111111110 2101001111 0010100110 0200000010 0111110221 1101130102 2201102220 0?11020011 1022111112 1201111031 0111102113 0110100110 1101311112 0001000200 1200011010 0111101 |
| *Crocidura russula* | 010??00000 210000a011 0110110?10 12101111?? 1?10001010 00????2112 000100?071 0000000010 2100111000 0010000000 100000001 0000000000 0011000000 1100110201 0111100000 1000011 |
| *Sorex araneus/californicus* | 0101?10??0 2010?00011 000011101? ??101111?? 1?1000111a 00????2112 000000?0?0 0000000010 2100011100 0210000000 1001001000 2000000000 0011000000 1100010001 0010100000 1000011 |
| *Erinaceus europaeus* | 0a1??a11a0 21a1000a00 0000110100 1211111101 1110000001 010000?102 000012?000 0000000010 010?010000 0000000000 0000000000 2?10000000 0000000002 01001002a0 0200000000 0?00211 |
| *Blarina brevicauda* | 010??10??0 20?0?00011 000011101? ??101111?? 1?20001010 00????2101 000000?0?0 0000000010 2110011000 0210000000 1001001000 ???0000000 0011000002 1100010001 0010100000 1000?11 |
| *Geotrypus antiquus* | 111??11111 1111001122 011011?1?2 1000100110 01121001?? 11???1??02 0???10??1? ???112?0?? 20??????22 02011?1?21 0111112213 11???????? 10???????? ?????????? ?????????? ??????? |

## Appendix 2

Character description (as in Sánchez-Villagra et al. 2006).

Note: An asterisk "*" indicates the character is additive or ordered. Some citations include "char. XX" to specify the character number used by the original authors to refer to the same or similar feature.

Dental characters

1. First lower incisor i1: 0 = absent; 1 = present. Coding for talpids except for *Scapanulus* follows Ziegler (1971). Coding for *Erinaceus* follows Gould (2001).

2. Third upper incisor I3: 0 = absent; 1 = present. Coding for talpids except for *Scapanulus* follows Ziegler (1971). Coding for *Erinaceus* follows Gould (2001). Following Ziegler (1971), *Urotrichus* and *Dymecodon* have an I3, but Imaizumi and Kubota (1978) argued that this tooth is missing in these two taxa. See Sánchez-Villagra et al. (2006) for alternative codings used in different analysis.

3. Third lower incisor i3: 0 = absent; 1 = present. Coding for talpids except for *Scapanulus* follows Ziegler (1971). Coding for *Erinaceus* follows Gould (2001). Following Ziegler (1971), *Urotrichus* and *Dymecodon* have an i3, but Imaizumi and Kubota (1978) argued that this tooth is missing in these two taxa. See Sánchez-Villagra et al. (2006) for alternative codings used in different analysis.

4. Upper dP1: 0 = absent; 1 = present. Coding for talpids except for *Scapanulus* follows Ziegler (1971).

5. Lower dp1: 0 = absent; 1 = present. Coding for talpids except for *Scapanulus* follows Ziegler (1971). According to Ziegler (1971), *Urotrichus* has a dp1, but Imaizumi and Kubota (1978) argued that this tooth is missing in this species. See Sánchez-Villagra et al. (2006) for alternative codings used in different analysis.

6. Upper P2: 0 = absent; 1 = present. Coding for talpids except for *Scapanulus* follows Ziegler (1971). Coding for *Erinaceus* follows Gould (2001).

7. Lower p2: 0 = absent; 1 = present. Coding for talpids except for *Scapanulus* follows Ziegler (1971). Coding for *Erinaceus* follows Gould (2001).

8. Upper P3: 0 = absent; 1 = present. Coding for talpids except for *Scapanulus* follows Ziegler (1971). Coding for *Erinaceus* follows Gould (2001).

9. Upper P3, number of roots: a = single-rooted; 1 = two or more roots.

10. Relative size (height and width) of first upper incisor and canine: 0 = first upper incisor larger; 1 = canine larger. See Jones and Manning (1992, figs 3 and 4), for illustrations useful to code this character. Besides own observations, the following references were checked: *Uropsilus* (Ellerman and Morrison-Scott 1966), *Scaptonyx* (Corbet and Hill 1992, p. 26, table 18), *Mogera* (Imaizumi 1970), *Parascaptor* (Corbet and Hill 1992), *Parascalops* (True 1896), *Scalopus* (True 1896; Gaughran 1954), and *Scapanus* (True 1896; Hartman and Yates 1985).

11. Upper P4, number of roots*: 0 = 1 root; 1 = 2 roots; 2 = 3 roots. The following taxa were coded following Hutchison (1968, p. 20, table 2): *Scaptonyx*, *Talpa europaea*, *Scaptochirus*, *Urotrichus*, *Neurotrichus*, *Scapanulus*, *Parascalops*, *Scalopus*, *Scapanus*, *Condylura*.

12. Upper canine C: 0 = absent; 1 = present.

13. Upper canine C, number of roots: 0 = 1 root; 1 = 2 roots. *Scaptonyx*, *Talpa europaea*, *Scaptochirus*, *Urotrichus*, *Neurotrichus*, *Scapanulus*, *Parascalops*, *Scalopus*, *Scapanus*, *Condylura* were coded following Hutchison (1968, p. 20, table 2), coding of *Erinaceus* follows Gould (2001, char. 19).

14. Second upper molar M2, relative height of buccal cusps: 0 = metacone > paracone; 1 = subequal or paracone > metacone. Coding for *Scapanus* is based on S. *townsendii* (BMNH).

15. Upper canine caniniform, with single posterior crest: 0 = posterior crest absent; 1 = posterior crest present. As shown by Witte (1997, figs 101–103), older individuals of *Talpa europaea* may lose the posterior crest and accessory cusp because of wear. Coding for *Scapanus* is based on S. *townsendii* (BMNH unnumbered).

16. Upper first molar M1, metacone is expanded posterolingually and approaches the position and function of a hypocone (Van Valen 1967): 0 = no; 1 = yes. Coding follows Van Valen (1967), who used the derived state of this character to diagnose the Scalopini (*Scapanus* + *Scalopus*).

17. Upper M2, distinct paraconule: 0 = absent; 1 = present. Thenius (1989, fig. 135) illustrated paraconules and metaconules in *Crocidura* sp., but they are not distinct in the specimens of C. *russula* examined in this work, so this species is coded as polymorphic (see also next character). Gould (2001, char. 114) recorded this feature as absent in all 16 specimens of *Erinaceus europaeus* she examined. Motokawa (2004, char. 37) coded this character, recording the paraconule as "absent" in many talpid species (e.g., *Uropsilus*, *Talpa europaea*, etc.) in which we recorded it as present.

18. Upper M2, distinct metaconule: 0 = absent; 1 = present. Coding of *Erinaceus* follows Gould (2001, char. 112).

19. First upper molar M1, mesostyle: 0 = absent; 1 = just one mesostyle visible; 2 = two mesostyles close to each other; 3 = two mesostyles separated by deep valley. We cannot be certain whether these three character states represent a logical sequence, and for that reason we leave it as non-additive.

20. Second upper molar M2, mesostyle: 0 = absent; 1 = just one mesostyle visible; 2 = two mesostyles close to each other; 3 = two mesostyles separated by deep valley. Motokawa (2004, char. 34) coded a similar character.

21. Second upper molar M2, relative length of metacrista and paracrista: 0 = metacrista longer than paracrista; 1 = subequal. See Storch and Qiu (1983).

22. "Anterior accessory cuspid (acc)" (Fig. 9; Hutchison 1968, fig. 6) or in other words, small mesial (anterior) discrete shelf (additional cuspule) to paraconid in lower m2: 0 = absent; 1 = present.

23. Distinctive anterior cingulum in lower molars m1-m2: 0 = absent; 1 = present. This feature may be the same as what Storch and Qiu (1983) called the precingulid in m1 when comparing *Urotrichus* (in which it is absent) with *Neurotrichus* (which has it).

24. Relative height of entoconid/metaconid in m1: 0 = metaconid > entoconid; 1 = subequal.

25. Talonid notch in m1/m2: 0 absent; 1 = present. See Storch and Qiu (1983) for data on this and related features in living and extinct talpids.

26. Cristid obliqua in m2: 0 = separated from posterior wall of trigonid by a notch; 1 = connected to posterior wall of the trigonid. Storch and Qiu (1983) discussed this and other related features of the lower molars of several living and extinct talpids.

27. Teeth red-tipped when unworn: 0 = no; 1 = yes.

28. Premolar row, when more than one upper premolar present (modified from Motokawa 2004; char. 19): 0 = crowded; 1 = gapped.

29. Contact of second upper incisor with first incisor (based on Motokawa 2004, char. 22): 0 = absent; 1 = present.

30. Height of the upper canine in contrast to that of the first incisor (modified from Motokawa 2004, char. 24)*: 0 = UC shorter than first incisor; 1 = subequal; 2 = taller.

31. Crown length versus width of the upper canine (based on Motokawa 2004, char. 25): 0 = subequal; 1 = crown length greater.

32. Crown height of the fourth upper premolar versus that of the upper canine (based on Motokawa 2004, char.

26)*: 0 = fourth upper molar shorter; 1 = subequal; 2 = fourth upper molar taller.

33. Crown length versus width of the fourth upper premolar (based on Motokawa 2004, char. 27): 0 = length greater or subequal; 1 = length smaller than width.

34. The parastyle of the fourth upper premolar (based on Motokawa 2004, char. 28): 0 = obvious; 1 = inconspicuous. Gould (2001, char. 63) found the parastyle in P4 of *Erinaceus europaeus* to be "weak" in two specimens and absent in 19. Dannelid (1998, fig. 6.4) labeled a parastyle in *Sorex araneus.*

35. The crown length of the second upper molar versus that of the first molar (based on Motokawa 2004, char. 31): 0 = subequal; 1 = smaller in the second upper molar.

36. Crown length of third upper molar versus that of the first molar (based on Motokawa 2004, char. 32): 0 = crown length of the third upper molar more than half than that of the first molar; 1 = less than half.

37. Crown area of third upper molar versus that of the fourth premolar (based on Motokawa 2004, char. 33): 0 = area of third upper molar subequal or larger; 1 = area of third upper molar smaller.

38. The metacingulum of the second upper molar (based on Motokawa 2004, char. 38): 0 = present; 1 = absent.

39. Posterior cingulum cusp of the second lower incisor (based on Motokawa 2004, char. 41): 0 = present; 1 = absent. This character is coded as missing in the soricids because of uncertainty about homologies in the lower dentition.

40. Anterior cingulum cusp of the fourth lower premolar (based on Motokawa 2004, char. 42): 0 = present; 1 = absent. This character is coded as missing in the soricids because of difficulties in homologizing this cusp of some talpids with any cusp of the soricids examined.

41. Posterior cingulum cusp of the fourth lower premolar (based on Motokawa 2004, char. 43): 0 = present; 1 = absent. Gould (2001, char. 192) coded this character for *Erinaceus europaeus* as absent in 23 of 24 specimens examined.

42. Lower premolar teeth (modified from Motokawa 2004, char. 44): 0 = crowded; 1 = gapped.

43. Crown length of the first lower molar versus that of the fourth premolar (based on Motokawa 2004, char. 45)*: 0 = subequal; 1 = greater in first lower molar; 2 = much greater (more than twofold).

44. Crown length of second lower molar versus that of first molar (based on Motokawa 2004, char. 47)*: 0 = smaller in second lower molar; 1 = subequal; 2 = greater in second lower molar.

45. Crown length of third lower molar versus that of first molar (based on Motokawa 2004, char. 48)*: 0 = much smaller and minute in third lower molar; 1 = subequal or smaller third lower molar; 2 = greater third lower molar.

46. Metastylid of second lower molar (based on Motokawa 2004, char. 49; see also Hutchison 1968, table 2, p. 20, fig. 6): 0 = absent; 1 = present.

47. Trigonid and talonid width of second lower molar: 0 = trigonid and talonid width subequal; 1 = trigonid width greater than talonid width.

## Cranial characters

48. Anterior nasal tip in lateral view (based on Motokawa 2004, char. 1)*: 0 = reaches the level of the incisors; 1 = the level of the canines; 2 = posterior to the posterior margin of the canines. Coding for *Scaptochirus* is 0 (contra Motokawa 2004).

49. The anterior extremity of the incisive foramen (based on Motokawa 2004, char. 2)*: 0 = anterior to the anterior margin of the second incisor; 1 = the level of the second incisor; 2 = reaches the level of the third incisor or posterior.

50. The anterior extremity of the palatine foramen (modified from Motokawa 2004, char. 3)*: 0 = reaches level of P4; 1 = reaches level of first molar; 2 = reaches level of second molar. Motokawa (2004) coded this character as we do in this work, but provided incomplete names for the character states. This mistake is corrected here.

51. Posterior margin of the anterior root of the zygomatic arch in ventral view ("anterior margin of the orbital region" of Motokawa 2004, char. 5; wording modified, same coding): 0 = extends to the second molar; 1 = extends to the third molar. For soricids, the anterior margin of the orbital region was considered to code this character.

52. Zygomatic arch: 0 = absent; 1 = present. Related to the absence of a zygomatic arch, the presence or absence of a jugal in soricids and talpids among eulipotyphlans is unclear, as reviewed by MacPhee and Novacek (1993). Hutchison (1976) listed the lack of jugal bone in the zygomatic arches as a condition characterizing all talpids, but Parker (1885, p. 178 and pl. 26) described and illustrated young stages of *Talpa europaea* with a jugal, while McDowell (1958) described the jugal as "slender" in talpids. The jugal is clearly present in *Erinaceus europaeus* (MacPhee and Novacek 1993; Mickoleit 2004).

53. Zygomatic arch (modified from Motokawa 2004, char. 6): 0 = shallow; 1 = deep (its height exceeds half the cranial height at a given position).

54. Lateral view of the zygomatic arch (modified from Motokawa 2004, char. 8): 0 = curved upwards; 1 = straight or slightly curved downwards.

55. In dorsal view, location of contact of zygomatic arch with braincase (based on Motokawa 2004, char. 10): 0 = lateral portion of the anterior margin of the braincase; 1 = medial to or at the middle point of the anterior margin

of the braincase. The character is defined differently by Motokawa (2004), but the implied conditions and the codings are the same as in that work.

56. The anterior face of the zygomatic arch (modified from Motokawa 2004, char. 12)*: 0 = extends to the first molar level; 1 = extends to second molar; 2 = extends to the third molar level; 3 = positioned posterior to the posterior margin or the third molar.

57. Position of posterior extremity of the auditory bulla in ventral view (based on Motokawa 2004, char. 15)*: 0 = anterior to the anterior process of the "mastoid process" (Motokawa 2004); 1 = in a similar position; 2 = posterior.

58. Anterior projection of mastoid ("mastoid process" sensu Motokawa 2004) (modified from Motokawa 2004, char. 17): 0 = well developed, projecting laterally; 1 = weakly developed or absent.

59. Dentary, upper sigmoid notch extension (based on Motokawa 2004, char. 51): 0 = upwards to the midline, between the uppermost portion of the lower base of the mandible and coronoid tip; 1 = subequal to that level.

60. The posterior tip of the angular process of the dentary (based on Motokawa 2004, char. 52)*: 0 = anterior to the condyle; 1 = similar; 2 = posterior to the condyle. *Galemys* is coded as "1" ("similar", e.g., BMNH 60.600, BMNH 8.8.4.4.4) and not as "0" as in Motokawa (2004).

61. Position of the mandibular condyle (based on Motokawa 2004, char. 54)*: 0 = below midline; 1 = midline, between the upper sigmoid notch and the coronoid tip; 2 = upwards towards the coronoid process.

62. Relative position of lacrimal foramen relative to infraorbital foramen: 0 = posterior to infraorbital foramen; 1 = just dorsal or dorsal at the level of the middle portion of infraorbital canal; 2 = dorsal, just anterior to anterior border of infraorbital canal. *Scaptochirus* is polymorphic for this character, the lacrimal foramen being either anterodorsal to anterior border (NRM A58 6714) or just dorsal (NRM A60 7786). In *Uropsilus* it is just dorsal (Hutchison 1968, p. 13, fig. 2A).

63. Foramina incisiva (sensu Koppers 1990): 0 = small, antero-posterior length shorter than length of M2; 1 = hypertrophied, antero-posterior length equal or longer than added length of two last upper molars.

64. Foramen "I" (Koppers 1990) in maxillary or in premaxillary-maxillary suture. 0 = absent; 1 = present. *Crocidura* and *Blarina* were coded following Koppers (1990, table 2).

65. Number of mental foramina, buccal side of dentary*: 0 = one; 1 = two; 2 = three of more. Variation for some taxa in this character was recorded. Three specimens of *Dymecodon pilirostris* show two foramina on each side (NSMT 27439, 27445, 27448), while one (NSMT 27450) has two on the left and three on the right side. While two foramina were recorded in *Euroscaptor micura* (NRM A591166), three were recorded in *E. mizura* NSMT 26693.

66. Mandibular angular process: 0 = rod-like; 1 = plate; 2 = knob. See Motokawa (2004, char. 53) for a similar character.

67. Anterior process of "mastoid process"*: 0 = above root of zygomatic arch; 1 = in line with root; 2 = below root of zygomatic arch. See below for a discussion about intraspecific variation in *Parascaptor leucura*.

68. Relative position of posterior border of infraorbital foramen to upper molar row*: 0 = anterior to or at border M1–M2; 1 = above, somewhere in M2 of border M2–M3; 2 = above, posterior to border M2–M3. For *Euroscaptor*, *E. longirostris* was coded for this character.

69. Relative position of anterior border (internal side) of zygomatic arch to upper molar row*: 0 = above, anterior to posterior end of M2; 1 = above, between border M2–M3 and posterior end of M3; 2 = above, posterior to M3.

70. Height of M1 crown at buccal side/dentary height in adults without much wear in their teeth: 0 = ratio typically below 1, 1 = ratio above 1. As mentioned by Thenius (1989, p. 89), some talpids (e.g., *Scalopus*) show a "partial" hypsodonty in their molars. Coding for this character should be considered as preliminary, and a more detailed study of hypsodonty in this group (as in Williams and Kay 2001) is recommended. *Scaptochirus moschatus* NRM.A600151 is an adult specimen with totally worn teeth and a value of 1.0. *Scapochirus* specimens with less wear in their teeth are characterized by higher values.

71. Fenestra ovalis shape: 0 = maximal/minimal diameter less than 2.5; 1 = maximal/minimal diameter more than 2.5. See Table 1 for absolute values of specimens measured. Segall (1970) provided stapedial ratio values for several taxa, including *Crocidura*, *Sorex*, *Erinaceus* (all 2.0), *Scalopus aquaticus* (2.5), and *Talpa europaea* (1.8).

72. Stapes footplate: 0 = not bullate; 1 = bullate (sensu Sánchez-Villagra and Nummela 2001). See Stroganov (1945) for illustrations of stapes relevant code of this character in *Desmana moschata*, *Talpa europaea*, *Mogera wogura*, *Scalopus aquaticus*, and *Scapanus latimanus*. Segall (1973) described several aspects of the ossicles of *Uropsilus soricipes*, and did not comment on any peculiarity of the stapes. We assume then that this species does not have a bullate stapes.

73. Bony canal surrounding stapedial artery traversing the stapedial foramen: 0 = absent; 1 = canal partially or totally ossified (see Sánchez-Villagra et al. 2006, fig. 10). Wilkie (1925) and Gaughran (1954, p. 26) reported a bony carotid canal traversing stapedial foramen for *Talpa europaea* and for *Scalopus*, respectively. In the specimen of *Desmana* (NRM A582793) used as basis to code this species, the cartoid canal traversing the stapedial foramen is only partially ossified. This feature is also discussed by

Segall (1970) for some talpids and some of the outgroups treated here.

Postcranial characters: shoulder region

74. Clavicle: 0 = elongated, in some cases with strong processes directed medio-ventrally; 1 = semirectangular, stout; 2 = quadratic (length clavicula = width). See Campbell (1939, figs 16–20).

75. Clavicle, "foramen for vein" (Campbell 1939 p. 5, figs 11–20): 0 = absent; 1 = present. *Urotrichus talpoides* is polymorphic for this character. The foramen is absent in NSMT 28208, 20619, 20620, 20623, but present in NSMT 20618.

76. Clavicle, articulations*: 0 = with scapula; 1 = with scapula and humerus; 2 = with just humerus. According to Moore (1986, p. 84), in *Uropsilus* the clavicle articulates with both the scapula and the humerus. Campbell (1939, fig. 21) illustrated a "humeral facet" in the clavicle of *Uropsilus.* This character replicates that of Sánchez-Villagra et al. (2004, char. 23) on the articulation of clavicle and humerus, and our codings are the same as those in that work for that character.

77. Tetrahedral heterotopic bone wedged in between the ventromedial spine of the clavicle and anterior basilateral portion of the manubrium (Hutchison 1968, p. 21): 0 = absent; 1 = present.

78. Scapula, suprascapular canal through the base of acromium (see Campbell 1939, figs 27–29): 0 = absent; 1 = present. The structure is a canal and not just a foramen; the two connected openings are at both sides of the base of the acromium. Specimens of some species examined have a foramen on just the side of the supraspinous fossa (e.g., *Talpa europaea* NRM A845474; *Condylura cristata* NRM A590531; *Sorex araneus* NRM A588784). Campbell (1939) reported the canal absent in *Galemys pyrenaicus*, but it is actually present in the specimens we examined of this species (NRM A594954), so we code this species as polymorphic.

79. Scapula, infraspinous fossa (following Campbell 1939; see also Reed 1951): 0 = absent; 1 = present. See Reed (1951, p. 537) for information on the reduction of the infraspinatus muscle in some species. This character is obviously correlated with Whidden's (2000) character 28.

80. Scapula, marked teres fossa (see Sánchez-Villagra et al. 2006, fig. 5; Campbell 1939, figs 22–31): 0 = absent; 1 = present. According to Reed (1951; p. 538), this feature is "presumably present in all talpids except *Uropsilus.*" This character is obviously correlated with Whidden's (2000) character 23.

81. Scapula, metacromium*: 0 = absent; 1 = present, small (length less than 1/3 length of the total spine); 2 = present, large (length equal to or more than 1/3 the full length of the spine). Campbell (1939, fig. 25) illustrated the scapula of a specimen of *Neurotrichus gibbsii* missing the metacromium, but Reed (1951; p. 537, fig. 3) reported this feature for this species. See Großmann et al. (2002) for an illustration of the metacromium in *Crocidura russula* and a discussion of its growth during ontogeny.

82. Scapula, coracoid process (= metacoracoid, Klima 1987) forms a distinctive process: 0 = does not form conspicuous process; 1 = conspicuous process. Ontogenetic data might lead to a reevaluation in the coding for some of the taxa, in which no trace of a suture or a clearly "separate" structure can be seen next to the glenoid fossa area (see Großmann et al. 2002).

83. Sternum, ventral surface: 0 = absence of distinct ridge; 1 = distinct ridge does not form a keel; 2 = prominent keel.

84. Sternum, proportions of manubrium*: 0 = manubrial length/width less than 1.5; 1 = between 1.5 and 3; 2 = between 3.0 and 4.5; 3 = more than 4.5. See Campbell (1939, p. 3, fig. 60, top) for data on this character; here he referred to "sternal," but surely meant manubrial.

Postcranial characters: vertebral column

85. Axis and C3, relation of neural spines: 0 = not ankylosed; 1 = ankylosed dorsally.

86. Axis, neural spine: 0 = simple knob; 1 = keel with cranio-caudal orientation.

87. C6 transverse process posterior extension (Horovitz and Sánchez-Villagra 2003, char. 19): 0 = does not reach border C7–T1; 1 = reaches or surpasses border C7–TI.

88. Number of caudal vertebrae*: 0 = equal or less than 14; 1 = more than 14, less than 20; 2 = 20 or more. Hutchison (1968) stated that in *Uropsilus soricipes* "there are at least 16 and probably a few more caudal vertebrae." We counted 20 in USNM-574297.

Humeral characters

89. "Deltoid process: 0 = absent; 1 = present as flange distal to the greater tuberosity; 2 = present as elongate hook on lateral edge of greater tuberosity. The deltoid process has often been the source of terminological confusion (Edwards 1937; Campbell 1939). In the shrew the deltoid process can be homologized with a short ridge on the lateral shaft of the humerus that lies distal to the greater tuberosity—a typically mammalian position. The hypertrophy of the greater tuberosity has caused in some talpids (e.g., *Neurotrichus*) the reduction of the deltoid process and in others (e.g., *Scapanus*) we can find it as an even larger element in the same relative position. Some authors have chosen instead to refer to the process at the distal end of the pectoral crest as the deltoid process (see char. 5) (e.g.,

Barnosky 1981; Geisler 2004)" (Sánchez-Villagra et al. 2004, char. 1).

90. "Position of humeral head: 0 = on posterior to posteromedial side of proximal end; 1 = lateral edge to center of head in line with lateral edge of shaft; 2 = medial edge of head in line with lateral edge of shaft; 3 = entire head lateral to lateral edge of shaft" (Sánchez-Villagra et al. 2004, char. 2).

91. "Orientation of humeral head: 0 = long axis of head parallel or subparallel to long axis of shaft; 1 = long axis of head at oblique angle to long axis of shaft" (Sánchez-Villagra et al. 2004, char. 3).

92. "Minimum width of humerus*: 0 = approximately 1/9–1/10th of the maximum length of humerus; 1 = approximately 1/7th; 2 = approximately 1/4–1/5th; 3 = approximately 1/3rd or less. The broadening and thickening of the humeral shaft reflects the physical stresses upon it and occurs in the more fossorial forms" (Sánchez-Villagra et al. 2004, char. 4).

93. "Distal end of pectoral crest: 0 = does not form pronounced and distinct process; 1 = forms pronounced and distinct process oriented proximo-medially" (Sánchez-Villagra et al. 2004, char. 5).

94. "Proximity of pectoral crest to lesser tuberosity: 0 = clear gap with a low proximal end of pectoral process; 1 = narrow gap or fused to form a bicipital tunnel. The tendon of origin of the M. biceps brachii passes through the bicipital groove. The plesiomorphic condition can be seen in *Uropsilus*, which is, according to Reed (1951, p. 543), the same as in *Sorex*: "In these forms the groove lies on the anterior face of the humerus between the pectoral ridge and the teres tubercle, as Campbell stated, but more important to its future development, the proximal part of it lies between the lesser tuberosity and the proximal end of the pectoral ridge" (Sánchez-Villagra et al. 2004, char. 6).

95. "Floor of bicipital groove: 0 = straight and parallel to long axis of humerus; 1 = displaced medially by pectoral crest near proximal end of humerus" (Sánchez-Villagra et al. 2004, char. 7).

96. "Open portion of proximal half of bicipital groove: 0 = visible in anterior view; 1 = visible in posterior view; 2 = not visible" (Sánchez-Villagra et al. 2004, char. 8).

97. "Pit for M. flexor digitorum profundus: 0 = absent, 1 = present" (Sánchez-Villagra et al. 2004, char. 10).

98. "Medial edge of trochlea: 0 = sharp, ventrally projecting ridge; 1 = straight or low ridge" (Sánchez-Villagra et al. 2004, char. 11).

99. "Lateral epicondyle: 0 = present as rounded protuberance; 1 = distal end forms laterally extended flange; 2 = lateral end has proximally directed hook; 3 = lateral end has spine-like proximally pointed hook" (Sánchez-Villagra et al. 2004, char. 12). We did not have humeri of these taxa available for examination, but based on Hutchison (1968; Fig. 11) and Campbell (1939, figs 35 and 41), *Scapanulus* and *Scaptonyx*, respectively, have either condition 2 or 3 for this character.

100. "Brachial fossa: 0 = small pit; 1 = cavernous excavation underlying greater tuberosity" (Sánchez-Villagra et al. 2004, char. 13).

101. "Crest between greater tuberosity and distal end of pectoral ridge: 0 = present; 1 = absent" (Sánchez-Villagra et al. 2004, char. 14).

102. "Trough between head of humerus and greater tuberosity: 0 = no groove/very shallow; 1 = deep groove" (Sánchez-Villagra et al. 2004, char. 15). Coding for *Galemys* is different from that in Sánchez-Villagra et al. (2004, char. 15), since there is a noticeable groove in BMNH 1960.10.11.5.

103. "Lesser tuberosity: 0 = in posterior view, inferior to proximal edge of head of humerus, 1 = in line with proximal edge of head or superior to head of humerus" (Sánchez-Villagra et al. 2004, char. 16).

104. "Head of humerus: 0 = round; 1 = elliptical. Talpids except *Uropsilus* show elliptical humeral heads, a condition associated with differences in the angles between the main axis of the humerus and the main axis of the humeral head (Reed 1951)" (Sánchez-Villagra et al. 2004, char. 17).

105. "Medial epicondyle builds proximally elongated flange or process: 0 = absent; 1 = present" (Sánchez-Villagra et al. 2004, char. 18).

106. "Greatest length of greater tuberosity and deltoid process: 0 = relatively short, approximately < 1/4 length of humerus; 1 = relatively long" (Sánchez-Villagra et al. 2004, char. 19).

107. "Pectoral crest: 0 = single straight process parallel to long axis of humerus; 1 = forms single curved process; 2 = long axis of humerus and pectoral crest having a perpendicular orientation (approximately 90°)" (Sánchez-Villagra et al. 2004, char. 20).

108. "Clavicular facet: 0 = absent; 1 = in lateral view wedge-shaped; 2 = rectangular; 3 = sharp ending" (Sánchez-Villagra et al. 2004, char. 26).

109. "Lateral side of capitulum: 0 = not noticeably elongated; 1 = laterally elongated so that capitulum has "football" shape" (Sánchez-Villagra et al. 2004, char. 28).

Hand characters

110. "Prepollex*: 0 = absent; 1 = present, just a knob; 2 = present, elongated, extending all along the scaphoid, but does not reach first metatarsal; 3 = present, extends to proximal portion of first metatarsal or beyond (os falciforme). Jullien (1967) reported and illustrated no prepollex in *Erinaceus* sp." (Sánchez-Villagra and Menke 2005, char. 1).

111. "Scaphoid and lunate*: 0 = not fused; 1 = fused: suture visible; 2 = fused, suture not visible. The difference between states 1 and 2 is like that found among some species of tupaiids (Sargis 2002, fig. 21)" (Sánchez-Villagra and Menke 2005, char. 2).

112. "Triquetrum, ulno-palmar expansion originating from distal portion: 0 = absent; 1 = present" (Sánchez-Villagra and Menke 2005, char. 3).

113. "Small sesamoid lateral to triquetrum: 0 = absent; 1 = present" (Sánchez-Villagra and Menke 2005, char. 4).

114. "Trapezium shape: 0 = distinctive distal arms absent; 1 = distinctive distal arms present. Most species coded with state 0 have a subtriangular trapezium in dorsal view, and only some species (e.g., *Scalopus aquaticus*, NRM A594978) are somewhat radially elongated" (Sánchez-Villagra and Menke 2005, char. 5).

115. "Isolated centrale: 0 = absent; 1 = present. Reed (1951, p. 553) reported that in soricids centrale and intermedium are not separate elements; Jullien (1967) reported and illustrated no centrale in *Erinaceus* sp." (Sánchez-Villagra and Menke 2005, char. 6).

116. "Pisiform forms a plate larger in area than the triquetrum and palmar to triquetrum, hamate and ulna: 0 = no; 1 = yes. In *Galemys pyrenaicus* the pisiform is large (and semitriangular), in *Desmana moschata* it is elongated and robust—in neither of these two species is the pisiform a large palmar plate" (Sánchez-Villagra and Menke 2005, char. 7).

Pelvis and sacrum characters

117. Fusion of acetabular area to vertebrae (Leche 1883): 0 = absent; 1 = present.

118. Fusion of posterior horizontal branch of ischion to vertebrae* (Leche 1883): 0 = absent; 1 = transverse processes expanded but not fused to ischion; 2 = fused.

119. Pubic approach: 0 = absent; 1 = present. Condition is scored as "1" when the space between left and right pubes is smaller than the width of the vertebral bodies at that level. This is not an actual pubic symphysis because it is located dorsal to the viscera (Leche 1883).

120. Pubic symphysis in the shape of a narrow bridge (Leche 1883): 0 = absent; 1 = present.

Hindlimb characters

121. Greater trochanter height: 0 = level with or below femoral head; 1 = higher than femoral head (see Sánchez-Villagra et al. 2006, fig. 11).

122. Third trochanter position: 0 = more distal than lesser trochanter; 1 = at the same level as lesser trochanter (see Sánchez-Villagra et al. 2006, fig. 11).

123. Tibial distal bridge (see Sánchez-Villagra et al. 2006, fig. 7, modified from Horovitz 2004, char. 124): 0 = absent; 1 = present. The proximal extensor retinaculum (part of the fascia known as the transverse annular ligament of the tarsus) is completely ossified in soricids.

124. Tibial falciform process (Reed 1951): 0 = absent; 1 = proximodistal blade; 2 = actual laterally projecting falciform process. The falciform process originates on the front side of the proximal end of the tibia.

125. Fibular lateral process (Reed 1951): 0 = absent; 1 = simple lateral process; 2 = process with proximal head; 3 = process with proximal and distal heads.

126. Fibular posterior process (Reed 1951): 0 = absent; 1 = present.

127. Astragalus process on lateral side of body (see Sánchez-Villagra et al. 2006, fig. 12): 0 = absent; 1 = present.

128: Astragalar head width (see Sánchez-Villagra et al. 2006, fig. 12): 0 = narrower than body; 1 = as wide as body or wider. The head width was measured on the head's maximum width, which in many cases is on a tilted plane, with the lateral side higher than the medial side.

129. Astragalar head, lateral side height relative to medial side: 0 = equal; 1 = lateral side higher.

130. Astragalar transverse ridge or groove posterior to trochlea (see Sánchez-Villagra et al. 2006, fig. 12): 0 = absent; 1 = ridge; 2 = groove.

131. Astragalar posteroventral groove (for the flexor fibularis muscle, also known as flexor digitorum profundus, see Sánchez-Villagra et al. 2006, fig. 12): 0 = shallow groove; 1 = deep groove or canal. The condition was scored as "1" when the groove was surrounded by raised medial and lateral sides.

132. Astragalar body shape* (see Sánchez-Villagra et al. 2006, fig. 12): 0 = mediolaterally wider; 1 = equal; 2 = anteroposteriorly longer. The anterior end of the astragalar trochlea was considered the anterior end of the body. The medial and lateral sides of the body did not include processes protruding beyond the trochlear ridges.

133. Astragalar medial trochlear ridge orientation (see Sánchez-Villagra et al. 2006, fig. 12): 0 = anteroposterior; 1 = posteriorly more lateral.

134. Anterior end of astragalar lateral trochlear ridge (modified from Horovitz 2004, char. 141; see Sánchez-Villagra et al. 2006, fig. 12): 0 = lateral trochlear ridge ends on the anterior end of the body; 1 = body is longer.

135. Astragalar medial plantar tuberosity (AMPT) protrudes medially beyond medial trochlear ridge (see Sánchez-Villagra et al. 2006, fig. 12): 0 = non-protruding; 1 = protruding.

136. Astragalar neck, angle with trochlea (see Sánchez-Villagra et al. 2006, fig. 12): 0 = small angle; 1 = large angle. The angle is smaller the more the trochlea and the

neck are aligned. This character is present in shrews, where the relationship between tibia and astragalus is somewhat different from that in most other eutherians: the trochlea is not in line with the major axis of the foot but is instead posteriorly more medial. This orientation involves a character complex including a tibia that displays a slanted distal facet (as visible in anterior view) to articulate with astragalus. In addition, the medial ridge of the astragalus is spherical to allow for flexion extension of the foot.

137. Astragalar posteroventral groove protrudes posteriorly in dorsal view: 0 = nonprotruding; 1 = protruding. The portion of the astragalus that is below the groove or ridge may protrude posteriorly beyond the trochlea in dorsal view.

138. Calcaneum sustentacular facet dimensions* (see Sánchez-Villagra et al. 2006, fig. 13): 0 = mediolaterally larger; 1 = round to square; 2 = proximodistally longer.

139. Calcaneum peroneal process distal extent: 0 = level with facet for cuboid; 1 = protrudes distally.

140. Calcaneum peroneal process lateral extent (see Sánchez-Villagra et al. 2006, fig. 13): 0 = does not protrude laterally; 1 = protrudes laterally.

141. Peroneal process position (see Sánchez-Villagra et al. 2006, fig. 13): 0 = lateral to calcaneocuboid facet; 1 = dorsolateral to calcaneocuboid facet. This character can be appreciated in distal view of the calcaneum.

142. Calcaneum facet for cuboid, major axis*: 0 = mediolaterally larger; 1 = equal axes; 2 = dorsoventrally larger; 3 = dorsoventrally much larger. All moles included here have a calcaneocuboid facet that is larger dorsoventrally than mediolaterally. *Galemys* and *Desmana* are extreme cases in this condition since their calcaneocuboid is very narrow and dorsoventrally long. A quotient of the mediolateral dimension over the dorsoventral dimension yielded values equal or smaller than 0.58 for the desmanines (character state "2") and values equal or larger to 0.67 for the remaining moles included here (character state "1").

143. Ectal facet concave on tuber calcis: 0 = absent; 1 = present. In soricides there is a posterior extension of the ectal facet onto the tuber calcis, forming a concave articular surface the posterior edge of which is raised.

144. Peroneal process and sustentaculum proximodistal lengths (see Sánchez-Villagra et al. 2006, fig. 13): 0 = peroneal process shorter; 1 = equal or peroneal longer.

145. Ectocuneiform medial canal: 0 = absent; 1 = present. This canal is visible in dorsal view as an incision on the medial side of the cuneiform.

146. Navicular facet for astragalus*: 0 = distal area larger; 1 = medial and distal equal; 2 = medial area larger. The navicular has a medial process that projects proximally, surrounding the astragalar head medially. The articular surface of this area of the navicular varies in size relative to the main (distal) articular area of the navicular.

147. Navicular ventral articular area size*: 0 = absent; 1 = ventral facet smaller than medial facet; 2 = ventral and medial facets subequal. In addition to the medial process of the navicular examined under character 34, there is, in some cases, a ventral-proximal process on the same bone that surrounds the astragalar head ventrally. The articular area of this process is compared here to that of the medial process.

148. Navicular shape in dorsal view: 0 = mediolaterally wider; 1 = proximodistally longer.

149. Cuboid medial proximal process (Horovitz 2004, char. 172): 0 = absent; 1 = present. This process extends from the proximal side of the cuboid medially and extends between the head of the astragalus and the navicular. This seems to be exclusive to moles among mammals (after taxa listed in Horovitz 2004). In many cases among talpids, the astragalus displays a groove to accommodate this process (e.g., *Scapanus*, see Sánchez-Villagra et al. 2006, fig. 6A).

150. Cuboid ventrolateral tunnel: 0 = absent; 1 = present. The ventral side of the cuboid (visible in lateral view) displays either a shallow sulcus or an almost enclosed canal (or tunnel) for the tendon of the m. peroneus longus.

151 Cuboid proximal surface proximodistal location relative to that of the navicular: 0 = equal; 1 = cuboid surface more distal.

152. Prehallux in contact with entocuneiform and navicular (Sánchez-Villagra and Menke 2005, fig. 8): 0 = absent; 1 = present. Some talpids have a prehallux or tibial sesamoid located medially and in contact with the entocuneiform and distal area of the navicular. Because of its position and relations, it is a serial homolog to the os falciforme or prepollex (a radial sesamoid), as discussed by Sánchez-Villagra and Menke (2005). In soricids, the prehallux when present is more distally placed; being also medial to the entocuneiform but not contacting the navicular, as in talpids. Since soricids do not have a prehallux in the same position as talpids, we coded them as "absent."

153. Length of Mt III relative to calcaneum*: 0 = much longer, at least 1.31-fold as long as the calcaneum; 1 = Mt III between 1.16 and 1.01-fold longer; 2 = shorter than calcaneum.

154. Mt IV distal extent relative to Mt III: 0 = about equal; 1 = Mt IV extends beyond Mt III.

155. Number of mammae*: 0 = 3 pairs; 1 = 4 pairs; 2 = 5 pairs. Codings were based on several sources: *Desmana* after Ognev (1962); *Parascalops*, *Scalopus*, *Scapanus* after Nowak (1999); *Neurotrichus* after Cabrera (1925, p. 93); *Urotrichus talpoides* and *Dymecodon pilirostris* after Imaizumi (1960); *Erinaceus* after Frost et al. (1991). Nowak (1999) claimed *Condylura* has eight pairs,

but he must have meant eight teats total and four pairs, which is what Fens (1988) reported. Ognev (1962, p.16) reported in *Talpa europaea* "usually six, sometimes eight teats present." The genus *Mogera* was reported by Imaizumi (1960) to have the formula $2 + 1 + 1 = 8$ or $1 + 2 + 1 = 8$ (= 4 pairs), whereas Yoshiyuki and Imaizumi (1991) reported for *Mogera etigo* "Mammae 10." See Table 1 (Sánchez-Villagra et al. 2006) for the absolute values used to code this character.

156. Position of nostrils (see Sánchez-Villagra et al., fig. 14): 0 = anterior; 1 = lateral; 2 = superior. The following taxa were coded following True (1896): *Neurotrichus*, *Parascalops*, *Scalopus*, *Scapanus*, and *Condylura*, while Imaizumi (1970) was followed for *Euroscaptor*, *Mogera*, *Urotrichus*, and *Dymecodon*. We follow True (1896, p. 48), who stated: "the nostrils are commonly stated to be 'supero-lateral' in *Scapanus* and superior in *Scalops*, but I am unable to discern any difference… they are superior in both." Abe et al. (1991, p. 48) stated that in *Mogera* (*Nesoscaptor*) *uchidae* the nostrils are "directed outward." Coding of *Erinaceus* follows Ade (1993), that of *Sorex araneus* and *Crocidura* (based on *C. bottegi*) follows Hutterer (1985).

157. Tail: 0 = scaly; 1 = not scaly.

## References


Abe, H., S. Shiraishi, and S. Arai. 1991. A new mole from Uotsurijima, the Ryukyu Islands. *Journal of the Mammalogical Society of Japan* 15: 47–60.

Aguilar, J.-P. 1982. Biozonation du Miocène d'Europe occidentale à l'aide des Rongeurs et corrélations avec l'échelle stratigraphique marine. *Comptes rendus de l'Académie des Sciences* 294: 49–54.

Böhme, M. 1996. Revision der oligozänen und untermiozänen Vertreter der Gattung *Palaeoleuciscus* Obrhelova, 1969 (Teleostei, Cyprinidae) in Mitteleuropa. Dissertation, Universität Leipzig.

Barnosky, A.D. 1981. A skeleton of *Mesoscalops* (Mammalia, Insectivora) from the Miocene Deep River Formation, Montana, and a review of the proscalopid moles: evolutionary, functional, and stratigraphic relationships. *Journal of Vertebrate Paleontology* 56: 1103–1111.

Bruijn, H. de, and C.G. Rümke. 1974. On a peculiar mammalian association from the Miocene of Oschiri (Sardinia). I and II. *Proceedings of the Koninklijke Nederlandse Akademie van Wetenschappen* B77: 44–79.

Cabrera, A. 1925. *Genera Mammalium*, vol. 2. Insectivora. Madrid: Galeopithecia (Museo Nacional de Ciencias Naturales).

Campbell, B. 1939. The shoulder anatomy of the moles. A study in phylogeny and adaption. *American Journal of Anatomy* 64: 1–39.

Corbet., G.B., and J.E. Hill. 1992. *The mammals of the Indomalayan region*. Oxford: Oxford University Press.

Crochet, J.-Y. 1974. Les insectivores des phosphorites du Quercy. *Palaeovertebrata* 6: 109–159.

Crochet, J.-Y. 1995. Le Garouillas et les sites contemporains (Oligocène, MP 25) des Phosphorites du Quercy (Lot, Tarn-et-Garonne, France) et leurs faunes de vertébrés—4. Marsupiaux et Insectivores. *Palaeontographica A* 236: 39–75.

de Blainville, H.M.D. 1840. Osteographie des mammifères insectivores (*Talpa*, *Sorex* et *Erinaceus* L.). In *Osteographie des mammifères (1)*. pp. 1–115. Paris: Baillère.

Dannelid, E. 1998. Dental adaptations in shrews. In *Evolution of shrews*, ed. Wojcik, J.M. and M. Wolsan. Bialowieza.

Edwards, L.F. 1937. Morphology of the fore-limb of the mole (*Scalops aquaticus*, L.) in relation to its fossorial habits. *The Ohio journal of science* 37: 20–41.

Ellerman, J.R., and T.C.S. Morrison-Scott. 1966. *Checklist of palaeoarctic and Indian mammals*, 2nd ed. 1758–1946. Oxford: Alden Press.

Fens, R. 1988. Insektenesser. In *Grizmeks Tierleben. Säugetiere*, vol. I. München: Kindler.

Fischer, G. 1813–1814. *Zoognosia tabulis synopticis illustrata*. Moscow: Nicolai Sergeidis Vsevolozsky.

Frost, D.R., W.C. Wozencraft, and R.S. Hoffmann. 1991. Phylogenetic relationships of hedgehogs and gymnures (Mammalia: Insectivora: Erinceidae). *Smithsonian contributions to zoology* 518: 1–69.

Gaughran, G.R.L. 1954. A comparative study of the osteology and myology of the cranial and cervical regions of the shrew, *Blarina brevicauda*, and the mole, *Scalopus aquaticus*. *Miscellaneous publications/Museum of Zoology, University of Michigan* 80: 1–82.

Geisler, J.H. 2004. Humeri of *Oligoscalops* (Proscalopidae, Mammalia) from the Oligocene of Mongolia. In *Tributes to Malcolm C. Mckenna: His Students, His Legacy*, ed. Gould, G.C., and S.K. Bell. *Bulletin of the American Museum of Natural History* 285: 166–176.

Gould, G.C. 2001. The phylogenetic resolving power of discrete dental morphology among extant hedgehogs and the implications for their fossil record. *American Museum novitates* 3340: 1–52.

Gregory, W.K. 1910. The orders of mammals. *Bulletin of the American Museum of Natural History* 37: 1–524.

Großmann, M., M.R. Sánchez-Villagra, and W. Maier. 2002. On the development of the shoulder girdle in *Crocidura russula* (Soricidae) and other placental mammals: evolutionary and functional aspects. *Journal of anatomy* 201: 371–381.

Hartman, G.D., and T.L. Yates. 1985. *Scapanus orarius*. *Mammalian Species* 253: 1–5.

Hermann, J. 1780. In *Geographische Geschichte des Menschen, und der allgemein verbreiteten vierfüßigen Thiere, nebst einer hierzu gehörigen zoologischen Weltcharte. vol. 2. Geschichte des Menschen, und der vierfüßigen Thiere*, ed. von Zimmermann, E.A.W. p. 6. Leipzig: Weygandsche Buchhandlung.

Horovitz, L. 2004. Eutherian mammal systematics and the origins of South American ungulates. In *Fanfare for an Uncommon Vertebrate Paleontologist: Papers on Vertebrate Evolution in Honor of Malcolm Carnegie McKenna*, ed. Dawson, M., and J. Lillegraven. *Bulletin of Carnegie Museum of Natural History* 36: 63–79.

Horovitz, L., and M.R. Sanchez-Villagra. 2003. A comprehensive analysis of marsupial higher-level relationships. *Cladistics* 19: 181–212.

Hugueney, M. 1972. Les talpidés (Mammalia, Insectivora) de Coderet-Bransat (Allier) et l'evolution de cette famille au cours de l'Oligocéne supérieur et du Miocéne inférieur d'Europe. *Documents des laboratoires de géologie de la Faculté des Sciences de Lyon* 50: 1–81.

Hutchison, J.H. 1968. Fossil Talpidae (Insectivora, Mammalia) from the later Tertiary of Oregon. *Bulletin of the Museum of Natural History* 11: 1–117.

Hutchison, J.H. 1974. Notes on type specimens of European Miocene Talpidae and a tentative classification of Old World Tertiary Talpidae (Insectivora: Mammalia). *Geobios* 7: 211–256.

Hutchison, J.H. 1976. The Talpidae (Insectivore, Mammalia): evolution, phylogeny, and classification. PhD Thesis, University of California, Berkeley.

Hutterer, R. 1985. Anatomical adaptations on shrews. *Mammalian Review* 15: 43–55.

Hutterer, R. 2005. Order Soricomorpa. In *Mammal species of the world. A taxonomic and geographic reference* (1), 3rd ed. Don E. Wilson and DeeAnn M. Reeder, 220–231. Baltimore: Johns Hopkins University Press.

Imaizumi, Y. 1960. *Coloured illustrations of the mammals of Japan* [in Japanese]. Osaka: Hoikusha.

Imaizumi, Y. 1970. *The handbook of Japanese land mammals*, vol. I. Tokyo: Shin-Schicho-Sha.

Imaizumi, Y., and K. Kubota. 1978. Numerical identification of teeth in Japanese shrew-moles, *Urotrichus talpoides* and *Dymecodon pilirostris*. *Bulletin of the Tokyo Medical and Dental University* 25: 91–99.

Jones, J.K., and R.W. Manning. 1992. *Illustrated key to skulls of genera of north American land mammals*. Lubbock: Texas Tech University Press.

Jullien, R. 1967. Musculature du member anterieur chez les principaux types d'Insectivores. *Mémoires du Muséum national d'Histoire naturelle* 48: 1–68.

Kindahl, M. 1957. Notes on the tooth development in *Talpa europaea*. *Arkiv för Zoologi* 11: 187–191.

Klima, M. 1987. Early development of the shoulder girdle and sternum in marsupials (Mammalia: Metatheria). *Advances in anatomy, embryology and cell biology* 109: 1–91.

Koenigswald, W.V., and M. Wuttke. 1987. Zur Taphonomie eines unvollständigen Skelettes von *Leptictidium nasutum* aus dem Ölschiefer von Messel. *Geologisches Jahrbuch Hessen* 115: 65–79.

Koppers, D. 1990. Vergleichende anatomisch-systematische Untersuchungen an Schädeln von *Talpa europaea* und anderen Insectivoren. *Zoologische Jahrbücher, Abteilung für Anatomie und Ontogenie der Tiere* 120: 109–125.

Lavocat, R. 1951. *Révision de la faune des mammiféres oligocénes d'Auvergne et du Velay*. Paris: Sciences et Avenir.

Leche, J.W.E.G. 1883. Zur Anatomie der Beckenregion bei Insectivora, mit besonderer Berücksichtigung ihrer morphologischen Beziehungen zur derjenigen anderer Säugethiere. *Kunglig Svenska vetenskaps-akademien Handlingar* 20: 1–113.

Linnaeus, C. 1758. *Systema naturae per regna tria naturae, secundum classes, ordines, genera, species, cum characteribus, differentiis, synonymis, locis*, 10th ed, vol. 1. Stockholm: Laurentii Salvii.

MacPhee, R.D.E., and M.J. Novacek. 1993. Definition and relationships of Lipotyphla. In *Mammal Phylogeny. Placentals*, ed. Szalay, F.S., M.J. Novacek, and M.C. McKenna. New York: Springer-Verlag.

Mayr, G., M. Poschmann, and M. Wuttke. 2006. A nearly complete skeleton of the fossil galliform bird *Palaeortyx* from the late Oligocene of Germany. *Acta Ornithologica* 41: 129–135.

McDowell, S.B. 1958. The greater antilles insectivores. *Bulletin of the American Museum of Natural History* 115: 113–214.

Mertz, D.F., P.R. Renne, M. Wuttke, and C. Mödden. 2007. A numerically calibrated reference level (MP28) for the terrestrial mammal-based biozonation of the European Upper Oligocene. *International Journal of Earth Science* 96: 353–361.

Mickoleit, G. 2004. *Phylogenetische Systematik der Wirbeltiere*. München: Pfeil Verlag.

Mitgutsch, C., M.K. Richardson, J. Rafael, J.E. Martin, P. Kondrashov, M.A.G. de Bakker, and M.R. Sánchez-Villagra. 2011. Circumventing the polydactyly 'constraint': the mole's 'thumb'. *Biology Letters* 8: 74–77. doi:10.1098/rsbl.2011.0494.

Mörs, T., and D. Kalthoff. 2010. A new species of *Amphilagus* (Mammalia: Lagomorpha) from the Late Oligocene lake deposits of Enspel (Westerwald, Germany). *Palaeobiodiversity and Palaeoenvironments* 90: 83–98.

Mörs, T., and W.V. Koenigswald. 2000. *Potamotherium valletoni* (Carnivora, Mammalia) aus dem Oberoligozän von Enspel im Westerwald. *Senckenbergiana Lethaea* 80: 257–273.

Moore, D.W. 1986. *Systematic and biogeographic relationships among the Talpinae (Insectivora: Talpidae)*. PhD dissertation, University New Mexico, Alburquerque.

Motokawa, M. 2004. Phylogenetic relationships within the family Talpidae (Mammalia: Insectivora). *Journal of Zoology London* 263: 147–157.

Nowak, R.M. 1999. *Walker's mammals of the world*, 6th edn. Baltimore: John Hopkins University Press.

Ognev, S.I. 1962. *Mammals of Eastern Europe and Northern Asia. Insectivora and Chiroptera*, vol. 1. Jerusalem: Sivan Press.

Parker, W.K. 1885. On the structure and development of the skull in the mammalia. *Philosophical transactions of the Royal Society of London* B176: 121–275.

Pomel, A.N. 1848. Etude sur les carnassiers insectivores. Première parite. Insectivores fossiles. *Archives des Sciences Physiques et Naturelles* 9: 244–251.

Poschmann, M., T. Schindler, and D. Uhl. 2010. Fossil-Lagerstätte Enspel—a short review of current knowledge, the fossil association, and a bibliography. *Palaeobiodiversity and Palaeoenvironments* 90: 3–20.

Reed, C.A. 1951. Locomotion and appendicular anatomy in three soricoid insectivores. *The American Midland Naturalist* 45: 513–671.

Sánchez-Villagra, M.R., and S. Nummela. 2001. Bullate stapedes in some phalangeriform marsupials. *Mammalian Biology* 66: 174–177.

Sánchez-Villagra, M.R., and P.R. Menke. 2005. The mole's thumb—evolution of the hand skeleton in talpids (Mammalia). *Zoology* 108: 3–12.

Sánchez-Villagra, M.R., P.R. Menke, and J.H. Geisler. 2004. Patterns of evolutionary transformation in the humerus of moles (Talpidae, Mammalia): a character analysis. *Mammal Study* 29: 163–170.

Sánchez-Villagra, M.R., I. Horovitz, and M. Motokawa. 2006. A comprehensive morphological analysis of talpid moles (Mammalia) phylogenetic relationships. *Cladistics* 22: 59–88.

Say, T. 1823. *Account of an expedition from Pittsburgh to the Rocky Mountains performed in the years 1819 and '20, under the command of Major Stephen H. Long* (compiled by Edwin James, 2 vols). Philadelphia: H.C. Carey and I. Lea.

Sargis, E.J. 2002. Functional morphology of the forelimbs of Tupaiids (Mammalia, Scandentia) and its phylogenetic implications. *Journal of Morphology* 253: 10–42.

Schaller, O. 2007. *Illustrated veterinary anatomical nomenclature*, 2nd ed. Stuttgart: Enke Verlag.

Segall, W. 1970. Morphological parallelisms of the bulla and auditorr ossicles in some insectivores and marsupials. *Fieldiana-Zoology memoirs* 51: 169–205.

Schindler, T., and M. Wuttke. 2010. Geology and limnology of the Enspel Formation (Chattian, Oligocene; Westerwald, Germany). *Palaeobiodiversity and Palaeoenvironments* 90: 21–27.

Shinohara, A., K.L. Campbell, and H. Suzuki. 2003. Molecular phylogenetic relationships of moles, shrew moles and desmans from the New and Old Worlds. *Molecular Phylogenetics and Evolution* 27: 247–258.

Shinohara, A., S. Kawada, M. Yasuda, and L.B. Liat. 2004. Phylogenetic position of the Malaysian mole, *Euroscaptor micrura* (Mammalia: Eulipotyphla), inferred from three gene sequences. *Mammal Study* 29: 185–189.

Skoczén, S. 1966. Age determination, age structure and sex ratio in mole, *Talpa europaea* Linnaeus, 1758 populations. *Acta Theriologica* 11: 523–536.

Storch, G., and Z. Qiu. 1983. The Neogene mammalian faunas of Ertemte and Harr Obo in Inner Mongolia (Nei Mongol), China. 2. Moles-Insectivore: Talpidae. *Senckenbergiana lethaea* 64: 89–127.

Storch, G., B. Engesser, and M. Wuttke. 1996. Oldest fossil record of gliding in rodents. *Nature* 379: 439–441.

Stroganov, S.U. 1945. Morphological characters of the auditory ossicles of recent Talpidae. *Journal of Mammalogy* 26: 412–420.

Swofford, D.L. 2002. *PAUP: phylogenetic analysis using parsimony, version 4.0 beta 10*. Sunderland: Sinauer Associates.

Thenius, E. 1989. *Zähne und Gebiss der Säugetiere*. Berlin: Walter De Gruyter.

Tobien, H. 1939. Die Insektenfresser und Nagetiere aus der aquitanen Spaltenfüllung bei Tomerdingen (Ulmer Alb). *Berichte der Naturforschenden Gesellschaft zu Freiburg i. Br* 36: 159–180.

True, F.W. 1896. A revision of the American moles. *Proceedings of the United States National Museum* 29: 1–115.

Van den Hoek Ostende, L.W. 1989. The Talpidae (Insectivora, Mammalia) of Eggingen-Mittelhard (Baden-Württemberg, F.R.G.) with special reference to the *Paratalpa-Desmanodon* lineage. *Stuttgarter Beiträge zur Naturkunde*. 152: 1–29.

Van den Hoek Ostende, L.W. 2001. Insectivore faunas from the Lower Miocene of Anatolia—part 5: Talpidae. *Scripta Geologica* 122: 1–45.

Van den Hoek Ostende, L.W., and O. Fejfar. 2006. Erinaceidae and Talpidae (Erinaceomorpha, Soricomorpha, Mammalia) from the Lower Miocene of Merkur-Nord. *Beiträge zur Paläontologie* 30: 175–203.

Van Valen, L., 1967. New Paleocene insectivores and insectivore classification. *Bulletin of the American Museum of Natural History* 135: 217–284.

Walter, R. 2003. *Erdgeschichte. Die Entstehung der Kontinente und Ozeane*, 5th ed. Berlin: Walter De Gruyter.

Weigelt, J. 1927. *Rezente Wirbeltierleichen und ihre paläobiologische Bedeutung*. Leipzig: Max Weg.

Whidden, H.P. 2000. Comparative myology of moles and the phylogeny of the Talpidae (Mammalia, Lipotyphla). *American Museum Novitates* 3294: 1–53.

Williams, S.H., and R.F. Kay. 2001. A comparative test of adaptive explanations for hypsodonty in ungulates and rodents. *Journal of Mammalian Evolution* 8: 207–229.

Witte, G.R. 1997. *Der Maulwurf*. Magdeburg: Westarp Wissenschaften.

Wuttke, M., D. Uhl, and T. Schindler. (eds.) 2010. The Fossil-Lagerstätte Enspel—exceptional preservation in an Upper Oligocene maar. *Palaeobiodiversity and Palaeoenvironments* 90: 1–98.

Yoshiyuki, M., and Y. Imaizumi. 1991. Taxonomic status of the large mole from the Echigo Plam, central Japan, with description of a new species (Mammalia, Insectivora, Talpidae). *Bulletin of the National Museum of Nature and Science-Series A* 17: 101–110.

Ziegler, A.C. 1971. Dental homologies and possible relationships of recent Talpidae. *Journal of Mammalogy* 52: 50–68.

Ziegler, R. 1985. Talpiden (Mammalia, Insectivora) aus dem Orlenaium und Astaracium Bayerns. *Mitteilungen der Bayerischen Staatssammlung für Paläontologie und historische Geologie* 25: 131–175.

Ziegler, P.A. 1990a. *Geological atlas of Western and Central Europe*, 2nd edn. Bath: Geological Society Publishing House.

Ziegler, R. 1990b. Talpidae (Insectivora, Mammalia) aus dem Oberoligozän und Untermiozän Süddeutschlands. *Stuttgarter Beiträge zur Naturkunde B* 167: 1–81.

Ziegler, R. 1994. Bisher übersehene Insectivora (Mammalia) aus dem Untermiozän von Wintershof-West bei Eichstätt (Bayern). *Mitteilungen der Bayerischen Staatssammlung für Paläontologie und historische Geologie* 34: 291–306.

Ziegler, R. 1998. Wirbeltiere aus dem Unter-Miozän des Lignit-Tagebaues Oberdorf (Weststeirisches Becken, Österreich): 5. Marsupialia, Insectivora und Chioptera (Mammalia). *Annalen des Naturhistorischen Museums Wien* 99 A: 43–97.

Ziegler, R., T. Dahlmann, J.W.F. Reumer, and G. Storch. 2005. Germany. In *The fossil record of the Eurasian Neogene Insectivores* (Erinaceomorpha, Soricomorpha, Mammalia), Part I, ed. Lars W. van den Hoek Ostende, Constantin S. Doukas and Jelle W. F. Reumer. *Scripta Geologica Spezial Issue* 5: 61–98.